

## Molecular modelling of SdiA protein by selected flavonoid and terpenes compounds to attenuate virulence in *Klebsiella pneumoniae*

Idowu Jesulayomi Adeosun<sup>a</sup>, Itumeleng Baloyi<sup>a</sup>, Aimen K. Aljoundi<sup>b</sup>, Elliasu Y. Salifu<sup>b</sup>, Mohammed Auwal Ibrahim<sup>c</sup> and Sekelwa Cosa<sup>a,\*</sup>

<sup>a</sup>Department of Biochemistry, Genetics and Microbiology, University of Pretoria, Hatfield, South Africa; <sup>b</sup>Molecular Bio-computation and Drug Design Laboratory, School of Health Sciences, University of KwaZulu-Natal, Durban, South Africa; <sup>c</sup>Department of Biochemistry, Ahmadu Bello University, Zaria, Nigeria

\*CONTACT: Sekelwa Cosa. Department of Biochemistry, Genetics and Microbiology, University of Pretoria, Lynnwood Road, Private Bag X20, Hatfield, 0028, South Africa. Email: sekelwa.cosa@up.ac.za

### Abstract

*Klebsiella pneumoniae* is one of the perturbing multidrug resistant (MDR) and ESKAPE pathogens contributing to the mounting morbidity, mortality and extended rate of hospitalization. Its virulence, often regulated by quorum sensing (QS) reinforces the need to explore alternative and prospective antivirulence agents, relatively from plants secondary metabolites. Computer aided drug discovery using molecular modelling techniques offers advantage to investigate prospective drugs to combat MDR pathogens. Thus, this study employed virtual screening of selected terpenes and flavonoids from medicinal plants to interrupt the QS associated SdiA protein in *K. pneumoniae* to attenuate its virulence. 4LFU was used as a template to model the structure of SdiA. ProCheck, Verify3D, Ramachandran plot scores, and ProSA-Web all attested to the model's good quality. Since SdiA protein in *K. pneumoniae* leads to the expression of virulence, 31 prospective bioactive compounds were docked for antagonistic potential. The stability of the protein-ligand complex, atomic motions and inter-atomic interactions were further investigated through molecular dynamics simulations (MDS) at 100 ns production runs. The binding free energy was estimated using the molecular mechanics/poisson-boltzmann surface area (MM/PB-SA). Furthermore, the drug-likeness properties of the studied compounds were validated. Docking studies showed phytol possesses the highest binding affinity (-9.205 kcal/mol) while glycitein had -9.752 kcal/mol highest docking score. The MDS of the protein in complex with the best-docked compounds revealed phytol with the highest binding energy of -44.2625 kcal/mol, a low root-mean-square deviation (RMSD) value of 1.54 Å and root-mean-square fluctuation (RMSF) score of 1.78 Å. Analysis of the drug-likeness properties prediction and bioavailability of these compounds revealed their conformed activity to lipinski's rules with bioavailability scores of 0.55 F. The studied terpenes and flavonoids compounds effectively thwart SdiA protein, therefore regulate inter- or intra cellular communication and associated in virulence *Enterobacteriaceae*, serving as prospective antivirulence drugs.

**Keywords:** Antipathogenic; Enterobacteriaceae; intercellular communication; molecular modelling; molecular dynamics simulations; phytocompounds

## 1. Introduction

*Klebsiella pneumoniae* amongst other ESKAPE pathogens (*Enterococcus faecium*, *Staphylococcus aureus*, *Klebsiella pneumoniae*, *Acinetobacter baumannii*, *Pseudomonas aeruginosa* and *Enterobacter* species) often escapes the action of almost all available antibiotics (Boucher et al., 2009). The World Health Organization (WHO) ranked *K. pneumoniae* as critical priority pathogen for the first-hand antibiotic research and development (Talebi Bezin Abadi et al., 2019), due to the healthcare and community burden it imposes, coupled with high prevalence in multidrug-resistance (MDR) and as a leading cause of death (Ventola, 2015). *K. pneumoniae* has the ability to colonize the gastrointestinal system, nasopharynx, and skin causing a wide range of infections, ranging from minor to life-threatening (Tzouveleki et al., 2012). Urinary tract infections (UTIs), soft tissue infections, intra-abdominal infections, septicaemia, wound or blood infections, and pneumonia are examples of such illnesses (Adeosun et al., 2019). The high resistance to several classes of antibiotics, including the last line of resort has been implicated in its biofilm-forming potential.

Recalcitrance to antibiotics, biofilm-forming ability, persistent immune system defense and chronic infections are often linked to the pathogen's quorum sensing (QS) regulatory system also well accepted as bacterial cell-to-cell communication (Cadavid et al., 2018). This mechanism not only enhances bacterial pathogenesis but also improves their ability to severely infect and damage their host (Cosa et al., 2019). In Gram-negative bacteria (GNB), the transcriptional regulators belonging to the LuxR protein plays a pivotal role by detecting the presence of autoinducers (AIs) known as N-acyl-homoserine lactones (AHLs) (Pradeep et al., 2018). Some *Enterobacteriaceae* pathogens such as *Salmonella*, *Escherichia*, including *Klebsiella* do not possess the AHLs producing enzyme known as LuxI synthase. However, they recognize AHLs produced by other bacteria due to the presence of SdiA protein which encodes an orphan LuxR homologue (Pacheco et al., 2021). Likewise, in *K. pneumoniae* the LuxI homolog is not found, thus the organism neither generates AHLs signal molecules of their own, however since this pathogen possesses SdiA, rather also senses the AI-2 molecules produced by the mixed community genera (Tavío et al., 2010). An SdiA transcriptional regulator in *K. pneumoniae* has been linked to cell division and the expression of virulence factors such as antibiotic resistance and biofilm formation. In addition, fimbriae and curli have been shown to play a pivotal role in *K. pneumoniae* biofilm development (Pacheco et al., 2021). This consequently marks the SdiA as a potential therapeutic target due to its ability to bind AHL and AI-2 signalling molecules from other pathogens, allowing for the transcription of several virulence genes (Pacheco et al., 2021; Pradeep et al., 2018).

Studies such as Pacheco et al. (2021) and Ahmed et al. (2021) have validated the role of SdiA in the production of QS autoinducers in *K. pneumoniae* and other *Enterobacteriaceae*, as noticed in *enterohemorrhagic Escherichia coli* (EHEC), *Salmonella enteritica* (Cheng et al., 2022). The crystal structure of SdiA has been reported in *E. coli* as PDB ID: 4LFU, 4LGW, 2AVX (Almeida et al., 2016). Since some *Enterobacteriaceae* (with the exception of *Pantoea* and *Erwinia*) encodes the same SdiA protein and are implicated in QS signaling molecule production and modulation of virulence factors, 4LFU was used as a template to model the structure of *K. pneumoniae* SdiA, thereby serving as a prototypical in search for

antivirulence or antagonistic compounds to impede the inter communication and associated virulence activities.

Due to the above mentioned pathogens' ability to regulate the respective virulence by means of the signalling mechanism (Gopu & Shetty, 2016), impeding this system hypothetically renders the disease-causing pathogen(s) less or non-virulent, presenting novel management of various bacterial infections (Cadavid et al., 2018). The secondary metabolites from medicinal plants may be the next-generation magic bullet in efficiently modulating QS associated SdiA protein and the respective virulence factors (Koh et al., 2013). The phenomenon of most plants growing in settings with high bacterial population fosters them to devise protective mechanisms against phytopathogens. Plants conquer through generating secondary metabolites that mimic microbial signal molecules, to compete for the protein active sites, subsequently impasse the expression of virulence factors and or reduced pathogenicity (Koh et al., 2013). The antivirulence mechanism therefore suppresses the expression of key genes vital for infections, rather than exerting bactericidal effect and selective pressure (Cosa et al., 2020). Terpenes, flavonoids, alkaloids, saponins, glycosides, anthraquinones and sesquiterpenoids among others, are all secondary metabolites capable of thwarting signalling mechanisms, hindering the expression of virulence factors (Akinyede et al., 2020; Baloyi et al., 2019; Maroyi, 2017).

Terpenes, commonly known as terpenoids, are abundant and diversified natural phytochemicals present in several medicinal plants and are the vital component of essential oils. Terpenes of natural products provide medical benefits (Cox-Georgian et al., 2019) and have proven to be a rich source of medical breakthroughs (Bergman et al., 2019). Flavonoids, on the other hand, are a class of naturally occurring plant compounds from various parts of the plants associated with a broad spectrum of health-promoting effects with a wide range of pharmacological effects, including antimicrobial, anti-inflammatory, anti-mutagenic and anti-carcinogenic properties coupled with their capacity to modulate key cellular enzyme functions (Paczkowski et al., 2017; Panche et al., 2016). The intriguing characteristics of these compounds make them of significant interest, hence they were considered in this study.

The exploration of these bioactive phytochemicals as QS and virulence inhibitors through virtual screenings, allows for a rapid and economical selection of prospective target ligands from large libraries of molecules (Huggins et al., 2011). This further accelerates the time and reduces the cost of traditional drug development processes (Naqvi et al., 2018) as well as narrowing the amount of potential ligands to be tested *in vitro* for drug screening and drug ability. This study took advantage of computational research tools to evaluate the antivirulence potential of existing plant secondary metabolites known for their medicinal activities against SdiA transcriptional regulator in *K. pneumoniae*.

## **2. Materials and methods**

### **2.1. Sequence retrieval, template identification and homology modelling**

Sequence of the SdiA gene was retrieved from Kyoto Encyclopedia of Genes and Genomes database and searched against Protein Data Bank (PDB) proteins using NCBI-BlastP, following the method described by Ahmed et al. (2021). The SdiA from *Escherichia coli*

(A-chain) (PDB ID: 4LFU) was used as template structure for the generation of the 3D model of *Klebsiella pneumoniae* SdiA by using Swiss Model Webserver (Arnold et al., 2006).

### **2.2. Validation of the generated model**

Protein structure validation suite (PSVS) ver. 1.5 (available at [http://psvs-1\\_5-dev.nesg.org/](http://psvs-1_5-dev.nesg.org/)) was used to determine the quality of the generated model, which revealed important validation parameters such as PROCHECK, VERIFY3D and Ramachandran plot. Furthermore, ProSA-Web was used to validate the protein structure of the modeled SdiA, thereby providing information on the general quality of the input model structure. The secondary structure of the modeled SdiA protein was determined using PDBsum as described by (Laskowski et al., 2018).

### **2.3. Prediction of the conserved residues and domains**

Following the method described by Ahmed et al. (2021), the conserved residues of SdiA of *K. pneumoniae* was predicted by aligning its sequence with the sequences with the LuxR family proteins. These proteins include the LasR from *Pseudomonas aeruginosa*, CviR from *Chromobacterium violaceum* and SdiA from *Escherichia coli*. The conserved domains of SdiA of *K. pneumoniae* were predicted using conserved domain and protein classification tool available at NCBI server (<https://www.ncbi.nlm.nih.gov/cdd/>).

### **2.4. Prediction of the binding site**

The CASTp 3.0 server was used for predicting the binding pocket of modeled SdiA as described by Tian et al. (2018). The pocket with the highest area and largest volume was considered as the most probable binding pocket of SdiA.

### **2.5. Molecular docking**

Site specific molecular docking was carried out following the method previously described by (Baloyi et al., 2021) with slight modifications. The 2-dimensional structures of the terpenes and flavonoids investigated were retrieved from the PubChem chemical database and sketched using Canvas 3.5 before being exported to Maestro 11.5. Chemically correct models of the ligands and the modeled SdiA receptor structure were built using Schrodinger's ligprep and a protein preparation wizard prior to the docking studies. The grids were then docked using the Glide ligand docking module and the Glide receptor. For the prepared protein created using the protein grid generation module, all docking calculations were performed using AutoDock 4.0 and Grids (Schrodinger, LLC, New York, NY, USA). Water and metals were removed before optimizing the hydrogen bonds, necessitating

minimization and resulting in scores that mimicked the potential energy change when the protein and the compound became bonded based on hydrogen bonds. Molecular docking was carried out on 31 compounds from natural sources (S1 table) which included the terpenes, flavonoids and other classes of compounds against the modeled SdiA protein.

## **2.6. Molecular dynamics simulations**

### **2.6.1. System preparation and molecular dynamics simulation**

The three-dimensional structures of best-docked terpenes and flavonoids were obtained in SDF format from PubChem, and the structures were optimized using Avogadro software. The modeled SdiA structure was prepared for molecular dynamics simulation (MDS) using the UCSF Chimera software package (Pettersen et al., 2004). MarvinSketch 6.2.1, 2014, and Molegro Molecular Viewer (MMV) were used for the preparation of the ligand and to ensure that the ligands proper angles and hybridization state were displayed (Kusumaningrum et al., 2014; Thomsen & Christensen, 2006). AutoDock Tools GUI was used to describe the grid box at the catalytic site of the protein (Allouche, 2011). The Lamarckian Genetic algorithm was used to perform docking calculations (Oleg & Arthur, 2010). The prepared systems protonation states were optimized using Maestro Schrödinger (Madhavi Sastry et al., 2013), necessary hydrogen atoms were corrected, and capping neutral residues to ensure protein stability during the simulation. Cumulatively, nine terpenes and eight flavonoids' systems of each protein comprising of the enzyme were subjected to MDS using the Graphic Process Unit version of the AMBER18 software package (Lee et al., 2018).

The protein was parametrized by the FF14SB (Maier et al., 2015) force field integrated in the AMBER18 suit (Wang et al., 2004). The Link Edit and Parm (LEAP) module (Nikitin, 2014) of AMBER18 was then used to add hydrogens that are missing from the systems during preparation. Also this module neutralizes the system by the addition of counter ions such as Na<sup>+</sup> and Cl<sup>-</sup> after which the systems were solvated by suspending them in Transferable Intermolecular Potential with 3 Point (TIP3P) water box of size 8 Å. A complexed coordinates and topology files of the receptor-ligand binding are generated for subsequent processing. The systems were minimized for 2000 energy steps. Initial minimization of 1000 steps with steep descent was performed for all the systems with a restrain potential and then followed by another 1000 steps minimization by conjugate gradient algorithm without restrain. The systems were then gradually heated from 0 K to 300 K with a 5 kcal/mol A harmonic restraint potential in NTP ensemble using Langevin thermostat of collision frequency of 1/ps. All the systems were then equilibrated at 300 K for 500ps without restraint with a constant pressure at 1 bar using Berendsen barostat. SHAKE algorithm was used to restrain all hydrogen bonds (Gonnet, 2007).

MDS production of 100 ns was then performed without restrain on the systems with target coupling of 2 ps and constant pressure at 1 bar. Analysis of the trajectories and coordinates generated from the MDS run was carried out through the CPPTRAJ and PTRAJ modules (Roe & Cheatham, 2013) incorporated in AMBER18. The RMSD and RMSF were calculated for all the systems. Discovery studio version v19.10.18289 (Sundaresan & Tharini, 2018) and UCSF chimera were used to visualize the trajectories while Origin data version 6.0 tool (Seifert, 2014) was used to plot all graphs.

## 2.6.2. Binding free energy calculations

To estimate the binding interactions of the compounds to the modeled SdiA enzyme, binding free energy calculations were carried out using the Molecular Mechanics/Poisson-Boltzmann Surface Area (MM/PB-SA) method (Homeyer & Gohlke, 2012; Hou et al., 2011).

This approach has been widely employed and proven to be reliable in measuring binding free energies involved in protein-ligand complex formation. Moreover, MM/PBSA is mathematically represented as follows:

$$\Delta G_{\text{bind}} = G_{\text{complex}} - G_{\text{receptor}} - G_{\text{ligand}} \quad (1)$$

$$E_{\text{gas}} = E_{\text{int}} + E_{\text{vdw}} + E_{\text{ele}} \quad (2)$$

$$G_{\text{sol}} = G_{\text{GB/PB}} + G_{\text{SA}} \quad (3)$$

$$G_{\text{SA}} = \gamma \text{SASA} \quad (4)$$

where van der Waals and electrostatic interactions are represented as  $E_{\text{vdw}}$  and  $E_{\text{ele}}$  while  $E_{\text{gas}}$  denote gas-phase energy and  $E_{\text{int}}$  as internal energy. The solvation free energy denoted by  $G_{\text{sol}}$  represents the solvation free energy and can be decomposed into polar and nonpolar contribution states. The polar solvation contribution,  $G_{\text{GB/PB}}$ , is determined by solving the GB/PB equation, whereas,  $G_{\text{SA}}$ , the nonpolar solvation contribution is estimated from the solvent-accessible surface area determined using a water probe radius of 1.4 Å.

## 2.7. Drug likeness properties of studied terpenes and flavonoids

The physicochemical and pharmacokinetic properties of the hit compounds were analysed using the SwissADME web server (<http://www.swissadme.ch/index.php>) (Daina et al., 2017). The compound's smileys were retrieved from the PubChem database, inserted in the webserver to run and generate the predicted parameters. Lipophilicity, water solubility and medicinal chemistry of the hit compounds were determined. The drug-likeness properties of the compounds (Lipinski's, Ghose's, Veber's, Egan's and Muegge's rules) and the bioavailability scores of the compounds were computed.

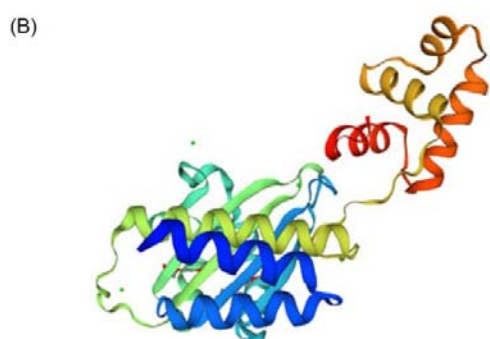
## 3. Results

### 3.1. Template identification and homology modelling

BLAST results showed 99.58% sequence similarity between SdiA protein in *Klebsiella pneumoniae* and the SdiA of the LuxR family transcriptional regulator (Accession number: KMI27310.1). The template 4LFU.1. A showed low E-value ( $1e - 158$ ) and a sequence identity of 64.58%, hence, it was selected as the template for modelling SdiA structure. The sequence alignment of SdiA target protein with 4LFU template protein, and the ribbon structure of the modeled SdiA protein are shown in Figure 1(A) and 1(B), respectively.

(A)

Model_01	MRDNDFFSWRRDMLHQFQSVAAAGEEVYNLLQRETEALEYDYYTLCVRHPVPFTRPRVTFQ	60
4lfu.1.A	MQDKDFFSWRRTMLLRFQRMETAEVYHEIELQAQQLEYDYSSLVCRHPVPFTRPKVAFY	60
	*:*:***** ** ;** : :.****: : : : *****;*****;*:*	
Model_01	STYPRAWMSHYQAENYFAIDPVLRPENFMRGHLPWEDGLFRDAAALWDGARDHGLKKGVT	120
4lfu.1.A	TNYPEAWVSYYQAKNFLAIDPVLNPNENFSQGHLMNNDLDFSEAQPLWEAARAHGLRRGVT	120
	:**.*:*	
Model_01	QCLTLPNHAQGFSLVSNANRLPGSYPDDELEMRLRMLTELSLLALLRLEDEMVMPPPEMKF	180
4lfu.1.A	QYLMLPNRALGFLSFSRCSAREIPILSDELQLKMQLLVRESLMALMRLNDEIVMTPEMNF	180
	* * **:* * **:* * . . ****: : : : * . **:*:*:*:*:* * **:*	
Model_01	SRRELEILKWTAEGKTSAEVAMILSISENTVNFHQKNMQRKFNAPNKTQIACYAVATGLI	240
4lfu.1.A	SKREKEILRWTAEGKTSAEIAMILSISENTVNFHQKNMQKINAPNKTQVACYAAATGLI	240
	*:* * **:* *****;*****;*****;*:*****;*****;*****	



**Figure 1.** (A) Alignment of template (4LFU) and model sequences. (B) 3D structure of SdiA model.

### 3.2. Validation of the generated model

The quality of the model was evaluated using PSVS that comprises assessment tools such as Ramachandran score, Verify3D, ProsaWeb and Molprobiy Clash score. The raw scores and Z-scores obtained for each parameter are shown in Table 1.

**Table 1. Assessment of the SdiA model structure using protein structure validation suite (PSVS).**

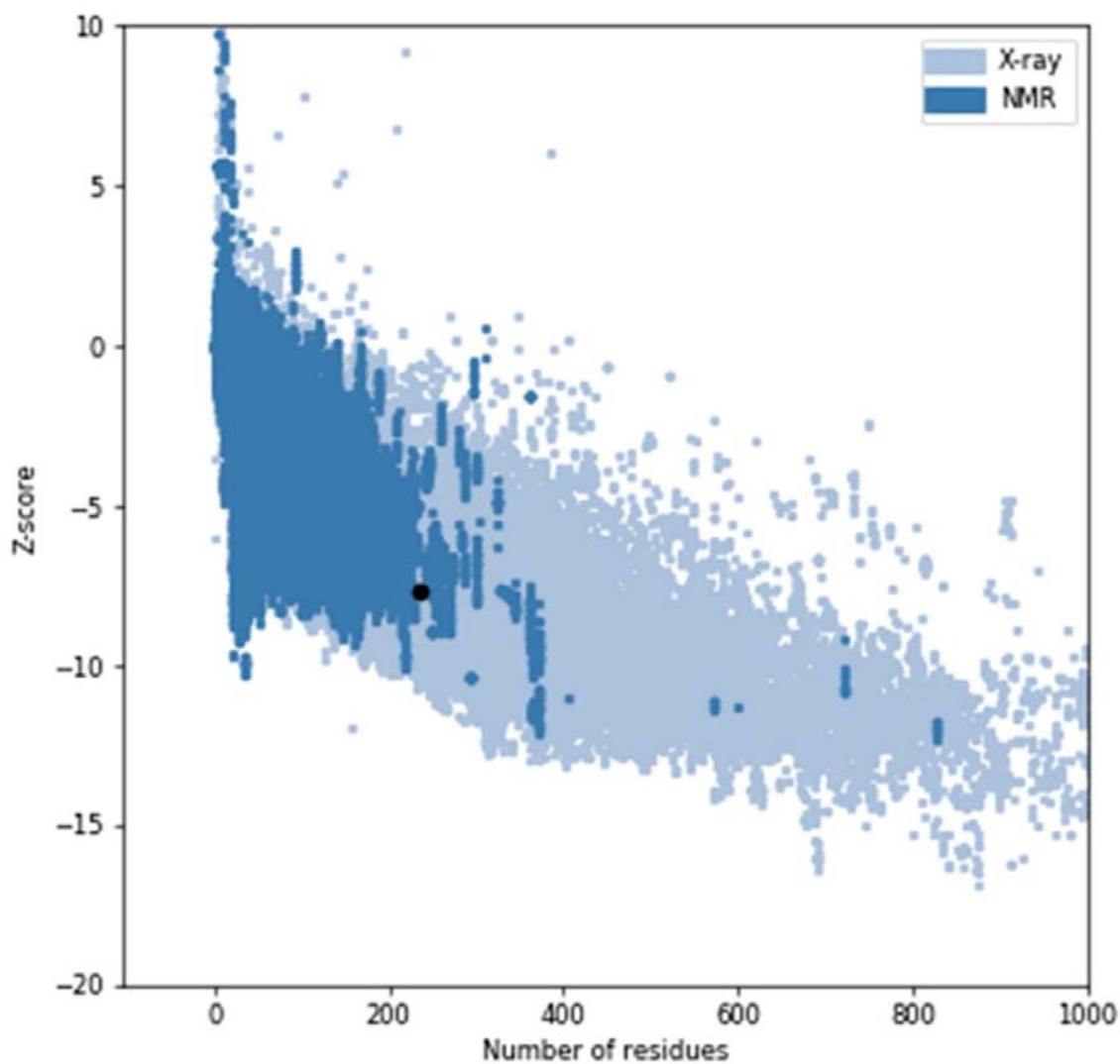
Parameter	Raw score	Z-score
Verify 3D	0.22	-3.85
Prosa11 (-ve)	0.92	1.12
Procheck (/w)	0.25	1.30
Procheck (all)	0.08	0.47
RMSD_bond length (Å)	0.015	-
RMSD_bond angle (°)	1.9	-
Molprobiy Clash score	2.21	1.15

Furthermore, Ramachandran plot scores from Procheck and Richardson’s lab showed that the selected model had 95.4% and 98.3% residues respectively in the favourable and allowed regions and no residue in outlier region (Table 2).

**Table 2. Assessment of model quality by Ramachandran plot scores.**

Ramachandran plot scores	Most favoured regions (%)	Generously and additionally allowed regions (%)	Disallowed regions (%)
Ramachandran plot scores (Procheck)	95.4	4.6	0.0
Ramachandran plot scores (Richardson's lab)	98.3	1.7	0.0

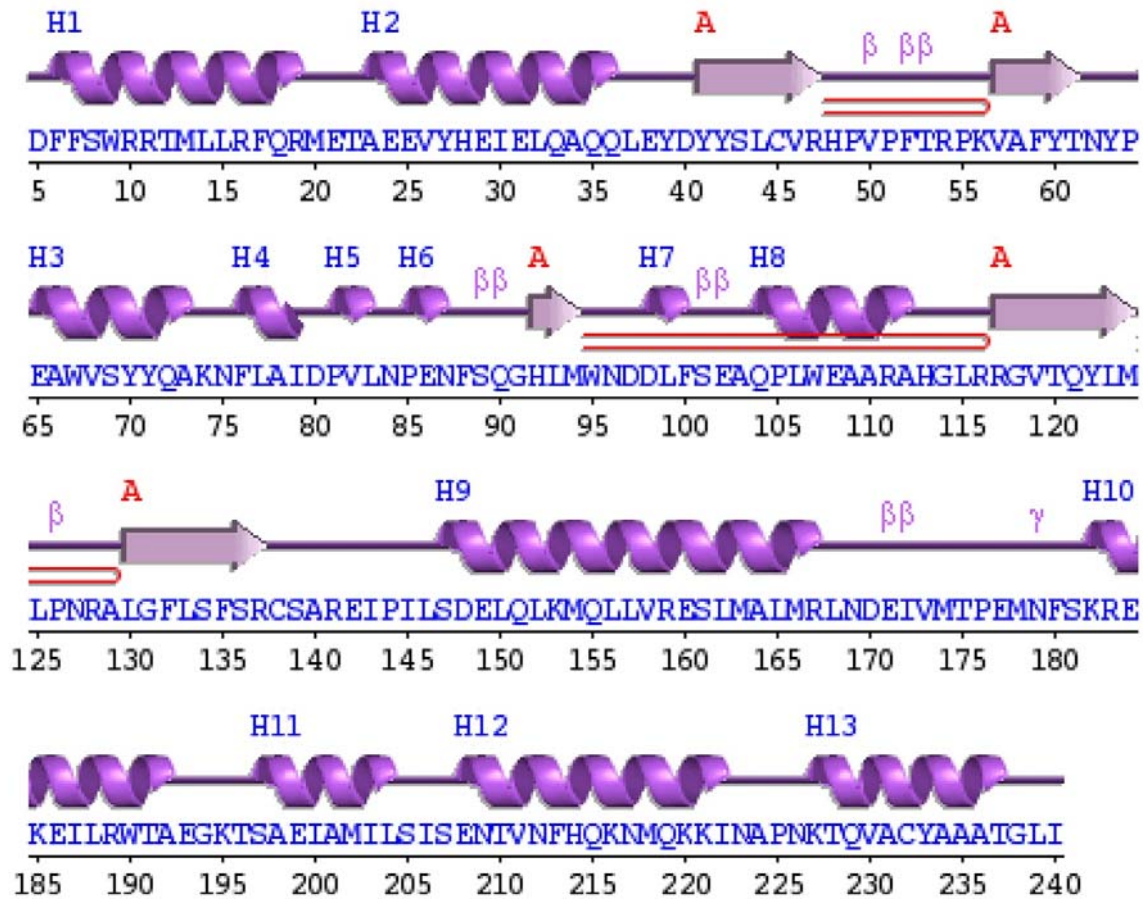
The ProsaWeb also revealed that the SdiA model protein had a Z-score of  $-7.66$ , thus confirmed the good quality of the model (Figure 2).



**Figure 2.** Validation of SdiA using ProSA web (Z-score =  $-7.66$ ).



In addition, validation of the model was performed based on the secondary structure using PDBsum. The result revealed that SdiA model had 13  $\alpha$ -helices which correspond with the X-ray crystal structure also having 13  $\alpha$ -helices (Figure 3).




**Figure 3.** Secondary structure prediction of SdiA model using PDBsum.

### 3.3. Analysis of the conserved residues and domains of SdiA

Multiple sequence alignment of SdiA (*Klebsiella pneumoniae*) with the conserved LuxR family proteins (CviR: *Chromobacterium violaceum*, LasR: *Pseudomonas aeruginosa* and SdiA: *Escherichia coli*) revealed that a good number of the amino acid residues in SdiA of *K. pneumoniae* were conserved (conserved areas indicated with asterisk\*) (S1 figure). Furthermore, analysis of the conserved domains of SdiA showed that it contains an autoinducer binding domain (24–156), a helix-turn-helix Lux regulon (180–234), C-terminal DNA-binding domain of LuxR-like proteins (180–235), DNA binding transcriptional regulator (180–240), DNA binding response regulator (175–240) and other domain hits (S2 figure).

**Table 3. Active site prediction of modeled SdiA protein through CASTp.**

(A)		
Name of the protein	Surface area (Å <sup>2</sup> )	Volume (Å <sup>3</sup> )
Regulatory protein SdiA	555.759	365.829
(B)	<b>(C) Amino acids located at the active site:</b> 43ser, 45cys, 54arg, 55pro, 56lys, 57val, 59phe, 61thr, 63tyr, 67trp, 68val, 70tyr, 71tyr, 72gln, 75asn, 76phe, 77leu, 80asp, 82val, 83leu, 94met, 95trp, 96asn, 97asp, 100phe, 106leu, 107trp, 109ala, 110ala, 111arg, 113his, 115leu, 116arg, 117arg, 118gly, 132phe, 134ser	
		

Key: (A) Area and volume of the active site; (B) 3D structure of the active site; (C) Amino acids located at the active site.

### 3.4. Analysis of the binding pocket of SdiA

CASTp 3.0 predicted binding pocket of SdiA with an area of 555.759Å<sup>2</sup> and volume of 365.829Å<sup>3</sup>. The amino acid residues lining the binding pocket were 43ser, 45cys, 54arg, 55pro, 56lys, 57val, 59phe, 61thr, 63tyr, 67trp, 68val, 70tyr, 71tyr, 72gln, 75asn, 76phe, 77leu, 80asp, 82val, 83leu, 94met, 95trp, 96asn, 97asp, 100phe, 106leu, 107trp, 109ala, 110ala, 111arg, 113his, 115leu, 116arg, 117arg, 118gly, 132phe, 134ser (Table 3).

### 3.5. Molecular docking of selected terpenes and flavonoids against SdiA protein

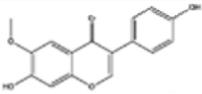
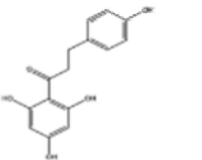
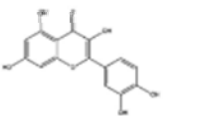
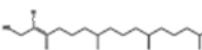
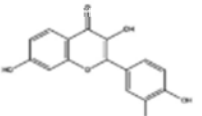
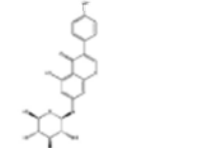
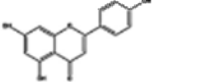
The *in silico* molecular docking results of the modeled SdiA protein against selected terpenes and flavonoids are shown in Table 4. The results of the docking analysis allowed for the determination of the best binding modes. In particular, the terpenes showed good potentials as bioactive antagonists or as quorum sensing inhibitors (QSIs) in *K. pneumoniae* SdiA (4LFU) protein.

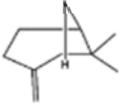
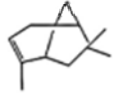
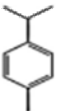
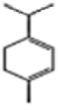

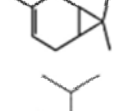

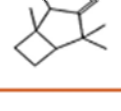
Based on these findings, terpenes possess high docking scores (Table 4) with a maximum score of -9.205 kcal/mol achieved by 3,7,11,15-tetramethyl-2-hexadecen-1-ol (phytol) comparable to the scores obtained for SdiA native ligand (AI-2 furanosyl borate diester) with a docking score of -6.081 kcal/mol. In addition to 3,7,11,15-tetramethyl-2-hexadecen-1-ol (phytol), eight (8) other terpenes: beta-pinene, alpha-pinene, 3-carene, sabinene, camphene, alpha-terpinene, p-cymene and isoterpinolene showed good docking scores between -7.473 kcal/mol and -7.039 kcal/mol (Table 4). These values (> -7 kcal/mol) were comparable to the obtained score of the AI-2 furanosyl borate diester (-6.081 kcal/mol), hence, they are regarded as terpenes showing good docking scores. The binding affinities of all 31 compounds are presented in S1 Table.

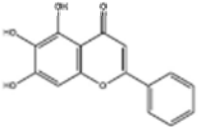
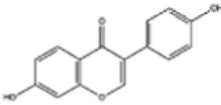
Flavonoids such as glycitein, phloretin, fisetin, genistin, apigenin, baicalein, daidzein and quercetin against the active site of SdiA protein in *K. pneumoniae* demonstrated improved binding affinities and possess high docking scores (Table 4). The maximum score of -9.752 kcal/mol achieved by glycitein, which was slightly higher than quercetin (-9.290 kcal/mol), a known QSI reference compound (Table 4). Daidzein showed the least docking score (-6.969 kcal/mol), although, comparable to the native ligand (-6.081 kcal/mol) (S1 Table).

The interaction networks between SdiA protein and the terpenes (Figure 4) revealed phytol (3,7,11,15-tetramethyl-2-hexadecen-1-ol) had sixteen hydrophobic interactions and formed hydrogen bonds with Val57 (Figure 4A). Whereas beta-pinene formed a polar interaction with HIS 113 and ten hydrophobic interactions (Figure 4B). Alpha pinene compound formed a polar interaction with HIS 113 and ten hydrophobic interactions (Figure 4C) while 3-Carene formed ten hydrophobic interactions (Figure 4D). Sabinene also formed polar interaction with HIS 113 (Figure 4E). Hydrophobic interactions were also observed in camphene, alpha-terpinene, p-cymene and isoterpinolene as shown in Figure 4. The native ligand, AI 2 furanosyl borate diester bound to the active site with hydrogen bonding to amino acids Arg111, Leu115, Arg116 and polar interaction with Asn96, Ser136 (Figure 4J).

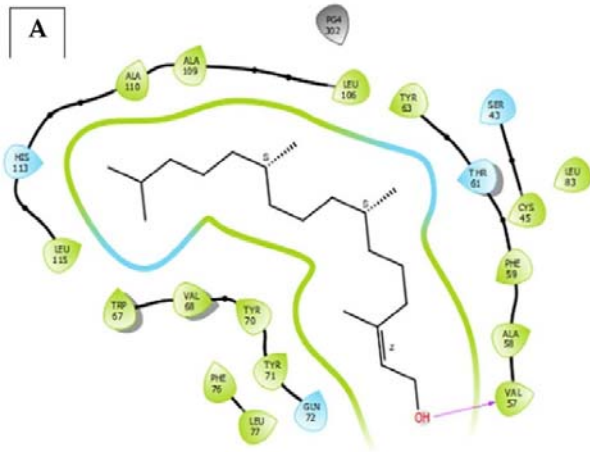
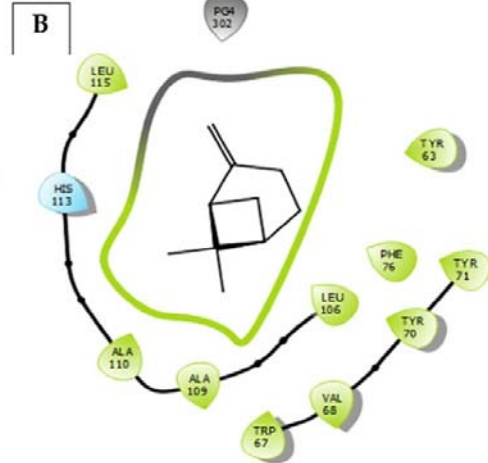
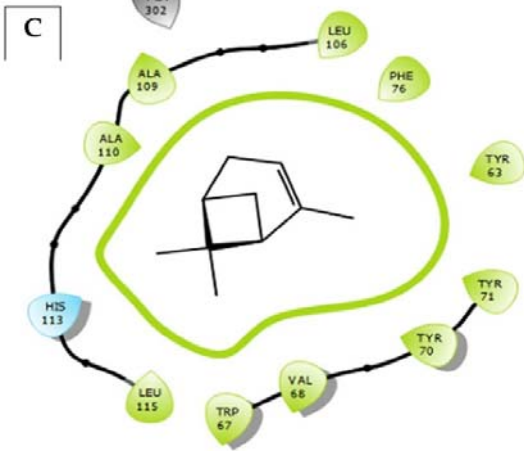
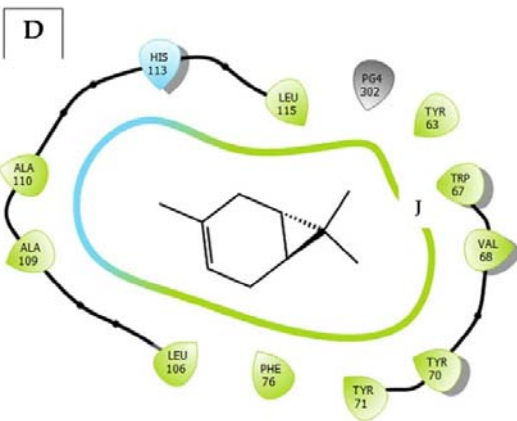
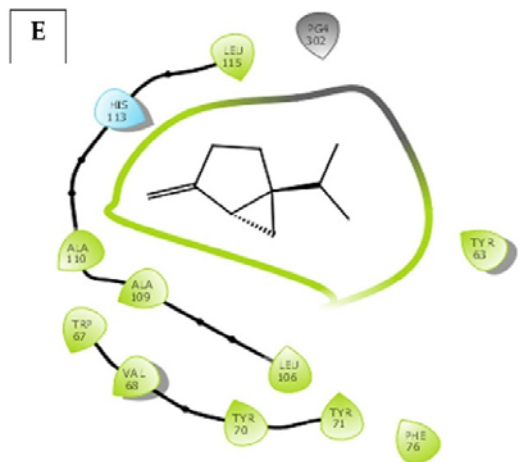
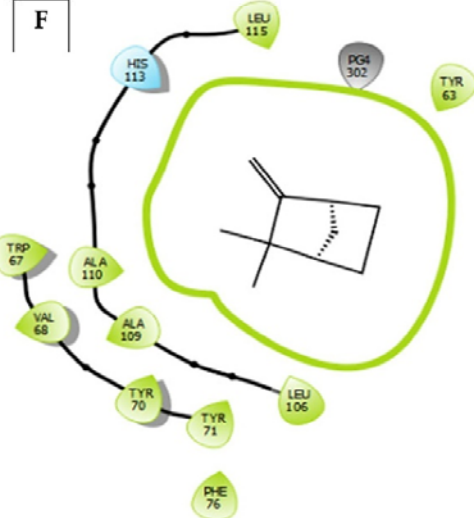
**Table 4. Molecular docking scores, root mean square deviation and fluctuations, binding free energy and drug-likeness prediction of best-docked terpenes and flavonoids.**

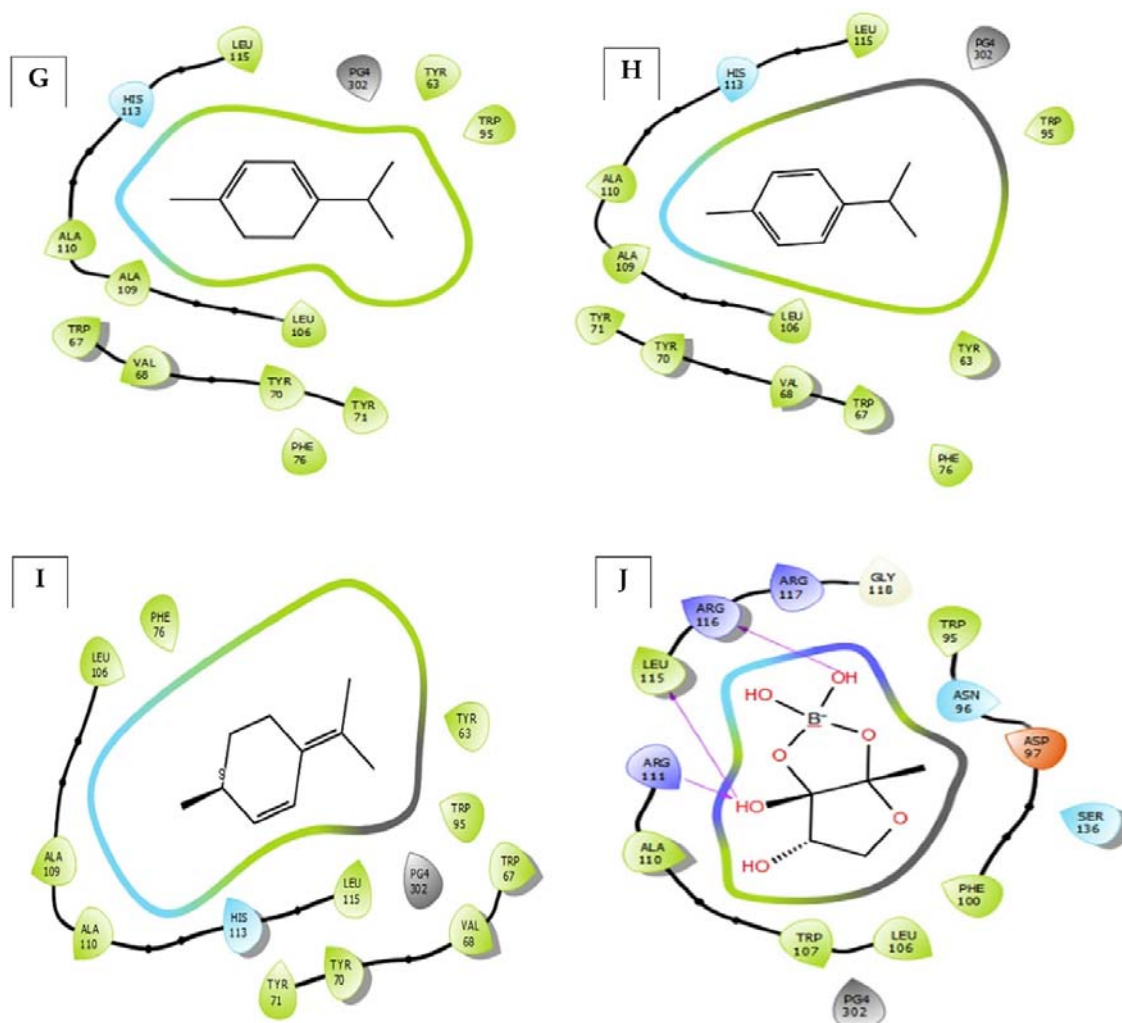
Compound name	Chemical structure	Molecular weight	Docking score (kcal/mol)	RMSD score (Å)	RMSF score (Å)	Binding energy (kcal/mol)	Drug likeness (Lipinski rule)
Glycitein (F)		284.26	-9.752	2.23	2.85	-30.3714	Yes; 0 violation
Phloretin (F)		274.27	-9.722	1.96	1.59	-28.8415	Yes; 0 violation
Quercetin (F)		302.236	-9.290	1.57	1.08	-37.1247	Yes; 0 violation
3,7,11,15-Tetramethyl-2-hexadecen-1-ol (phytol) (T)		296.5	-9.205	1.54	1.78	-44.2625	Yes; 1 violation: MLOGP > 4.15
Fisetin (F)		286.24	-8.364	1.71	2.09	-33.4770	Yes; 0 violation
Genistin (F)		432.4	-8.337	1.44	1.35	-68.1393	Yes; 1 violation: NH or OH > 5
Apigenin (F)		270.0528	-8.222	2.14	1.83	-40.9094	Yes; 0 violation

Compound name	Chemical structure	Molecular weight	Docking score (kcal/mol)	RMSD score (Å)	RMSF score (Å)	Binding energy (kcal/mol)	Drug likeness (Lipinski rule)
Beta-pinene (T)		136.23	-7.473	2.58	3.23	-21.4366	Yes; 1 violation: MLOGP > 4.15
Alpha-pinene (T)		136.23	-7.343	2.14	1.40	-19.1913	Yes; 1 violation: MLOGP > 4.15
P-cymene (T)		134.22	-7.277	2.21	1.92	-16.6186	Yes; 1 violation: MLOGP > 4.15
Alpha-terpinene (T)		136.23	-7.245	1.73	1.39	-19.2618	Yes; 0 violation
Isoterpinolene (T)		136.23	-7.235	1.61	2.10	-18.8961	Yes; 0 violation
3-Carene (T)		136.23	-7.226	2.09	1.53	-19.2745	Yes; 1 violation: MLOGP > 4.15
Sabinene (T)		136.23	-7.209	1.48	1.17	-19.3283	Yes; 1 violation: MLOGP > 4.15
Camphene (T)		136.24	-7.039	1.86	3.74	-19.8651	Yes; 1 violation: MLOGP > 4.15

Compound name	Chemical structure	Molecular weight	Docking score (kcal/mol)	RMSD score (Å)	RMSF score (Å)	Binding energy (kcal/mol)	Drug likeness (Lipinski rule)
Biacalein (F)		270.24	-6.996	1.54	1.56	-39.1342	Yes; 0 violation
Dalzein (F)		254.24	-6.969	1.69	2.05	-32.7409	Yes; 0 violation

Key: T = Terpene; F = Flavonoid.

**A****B****C****D****E****F**

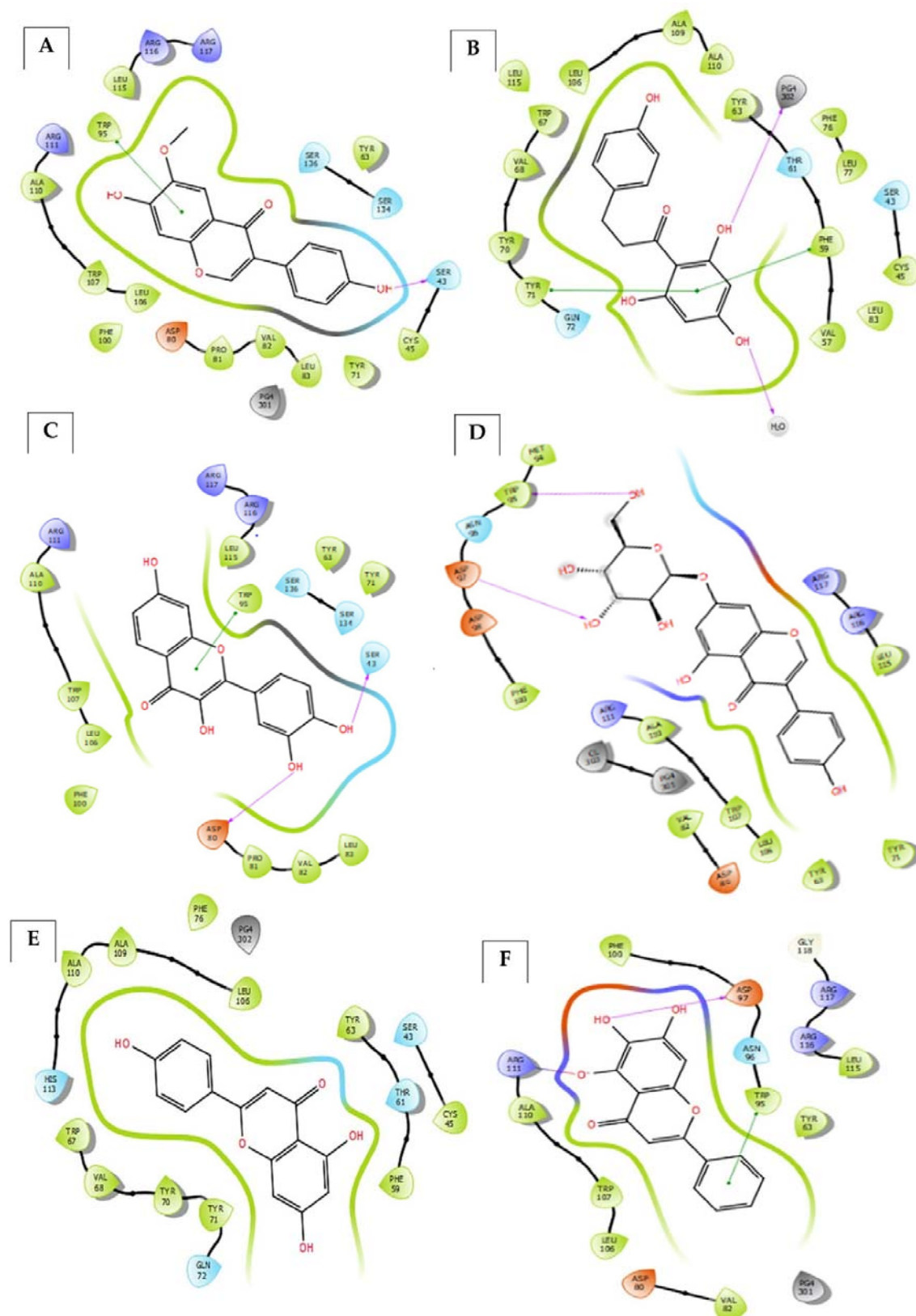


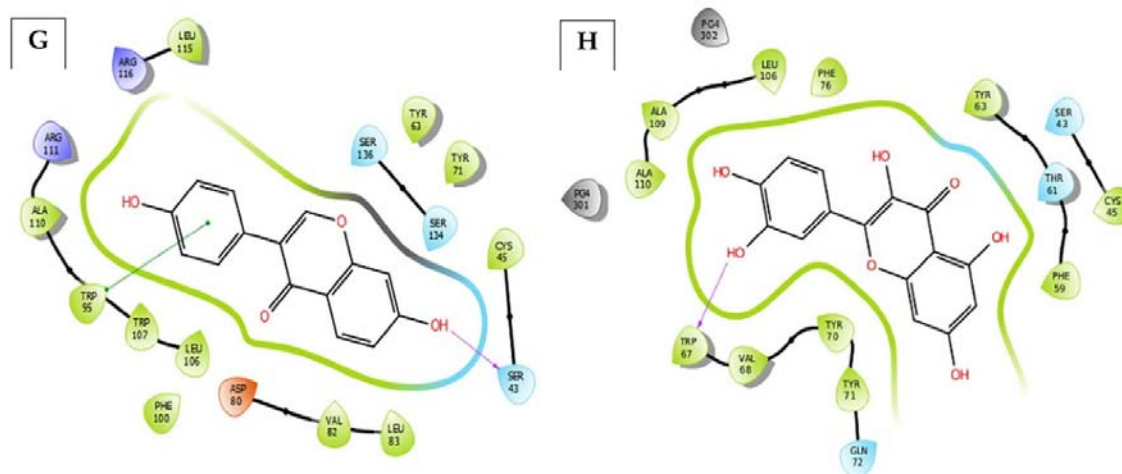
**Figure 4.** Interaction network between SdiA protein and terpenes showing good docking scores. The protein residues with a negative charge are shown in red, positive charge in velvet, polar in cyan, and hydrophobic in parrot green. The H-bond interactions are shown as a purple arrow, pi-pi stacking as a green line. (A) 3,7,11,15-tetramethyl-2-hexadecen-1-ol (phytol), (B) beta pinene, (C) alpha pinene, (D) 3-carene, (E) sabinene, (F) camphene, (G) alpha-terpinene, (H) p-cymene, (I) isoterpinolene, (J) furanosylborate diester (AI-2 molecule).

Docked flavonoid compounds against SdiA protein with respective interactions were as detailed in Figure 5. Glycitein had twelve hydrophobic interactions, hydrogen-bonded with Ser43 and a pi-pi stacking with Trp95 (Figure 5A) whereas phloretin formed hydrogen bonds with PG4 302 and H<sub>2</sub>O, a pi-pi stacking with Tyr71 and Phe59 and fifteen hydrophobic interactions (Figure 5B). Fisetin compound was also shown to form hydrogen bonds with Asp80 and Ser13 as well as fourteen hydrophobic interactions (Figure 5C) while genistin also formed hydrogen bonds with Asp97 and Trp 95 with ten hydrophobic interactions (Figure 5D). Apigenin had eleven hydrophobic interactions (Figure 2E) as well as baicalein having eight hydrophobic interactions, a pi-pi stacking with Trp95, a hydrogen bond with Asp97 and a salt bridge with Arg111 (Figure 5F). Daidzein formed a hydrogen bond with Ser43, pi-pi stacking with Trp95 and eleven hydrophobic interactions (Figure 5G). Quercetin actively



bound to the protein forming hydrogen bonds with Trp57, polar interactions with Gln72, Thr61 and Ser43 (Figure 5H).





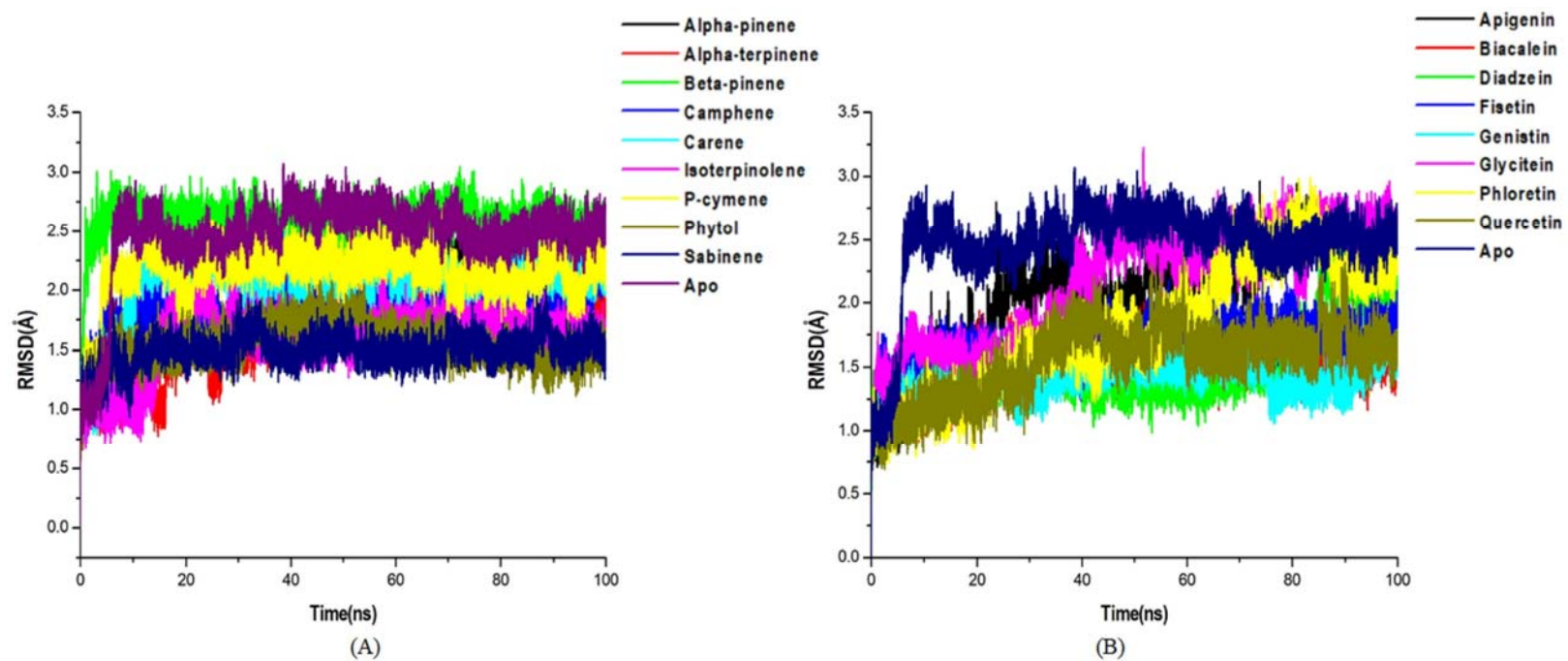
**Figure 5.** Interaction network between SdiA protein and flavonoids showing good docking scores. The protein residues with a negative charge are shown in red, positive charge in velvet, polar in cyan, and hydrophobic in parrot green. The H-bond interactions are shown as a purple arrow, pi-pi stacking as a green line. (A) Glycitein, (B) Phloretin, (C) Fisetin, (D) Genistin, (E) Apigenin, (F) Baicalein, (G) Daidzein, (H) Quercetin.

### 3.6. Dynamic conformational stability and fluctuations of the studied terpenes and flavonoid compounds

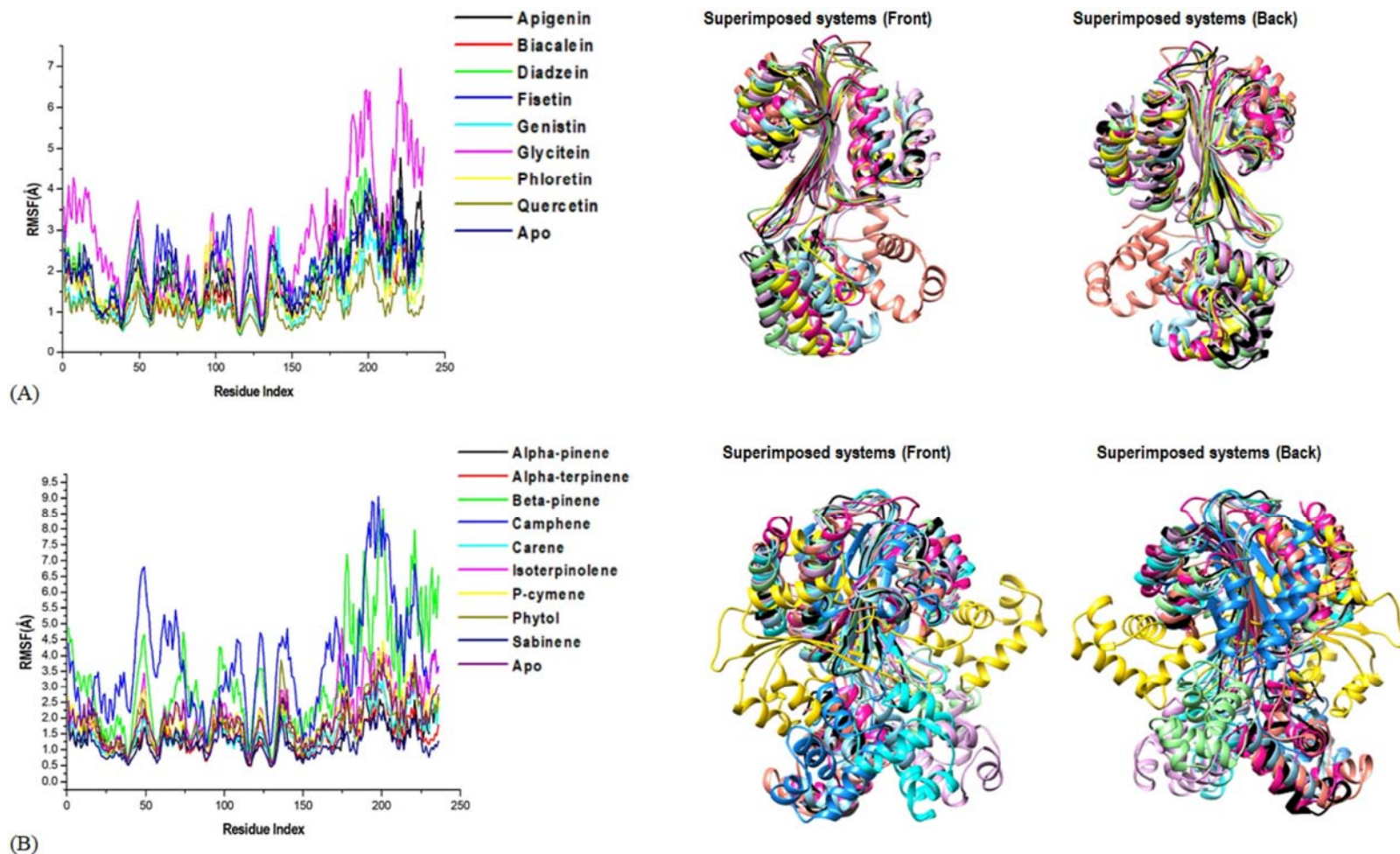
Further analysis of interactions of terpenes and flavonoids and MDSs were conducted to investigate their respective inhibitory performance in SdiA. Through validation of the system's stability, we can deduce disrupted motions and avoid artifacts that may arise during the simulation. In this study, root-mean-square deviation (RMSD) calculated to measure the systems' stability during the 100 ns simulations (Figure 6) were recorded as average RMSD values (Table 4).

For all frames of SdiA bonded terpene compounds systems, alpha-pinene, alpha-terpinene, beta-pinene, camphene, 3-carene, isoterpinolene, p-cymene, 3,7,11,15-tetramethyl-2-hexadecen-1-ol (phytol), sabinene and the unbound SdiA (Apo) revealed RMSD values of 2.14 Å, 1.73 Å, 2.58 Å, 1.86 Å, 2.09 Å, 1.61 Å, 2.21 Å, 1.54 Å, 1.48 Å, and 2.50 Å respectively. The comparative C- $\alpha$  RMSD plots showing the degree of stability and convergence of the studied systems over the 100 ns MDS time is shown in Figure 6(A).

On the other hand, the recorded average RMSD values for all frames of SdiA bonded flavonoids which include apigenin, biacalein, diadzein, fisetin, genistin, glycitein, phloretin, quercetin and unbound SdiA (Apo) were 2.14 Å, 1.54 Å, 1.69 Å, 1.71 Å, 1.44 Å, 2.23 Å, 1.96 Å, 1.57 Å, and 2.50 Å, respectively (Table 4). The comparative C- $\alpha$  RMSD plots showing the degree of stability and convergence of the studied systems over the 100 ns MDS time is shown in Figure 6(B).



**Figure 6.** Comparative C- $\alpha$  RMSD plots showing the degree of stability and convergence of the studied terpene compounds (A) and flavonoids (B) over the 100 ns molecular dynamics simulation time.



**Figure 7.** The time evolution RMSF of each residue of the protein C $\alpha$  atom over 100 ns for the studied flavonoids (A) and terpenes (B) superposed on the crystal structures of the studied systems to show differences in fluctuations and conformational changes. Comparative C $\alpha$  RMSF plot showing the degree of major flexibility of certain loops and helices at the highest fluctuation during the simulation.

The time evolution root-mean-square fluctuation (RMSF) of each residue is indicative of the differences in fluctuations of conformational changes of the protein C $\alpha$  atom over 100 ns for the studied systems (selected terpenes and flavonoids) was superposed on the crystal structures of the studied systems (Figure 7).

The evolution of protein structure flexibility upon ligand binding probes residue performance and their association with the ligand during MD simulation. The complexes (SdiA bonded terpenes and flavonoids) residual fluctuations were evaluated using the RMSF algorithm to assess the effect of inhibitor binding towards the respective targets over 100 ns simulations. The computed average atomic fluctuation of the terpenes which include alpha-pinene, alpha-terpinene, beta-pinene, camphene, 3-carene, isoterpinolene, p-cymene, 3,7,11,15-tetramethyl-2-hexadecen-1-ol (phytol), sabinene and the unbound SdiA (Apo) were 1.40 Å, 1.39 Å, 3.23 Å, 3.74 Å, 1.53 Å, 2.10 Å, 1.92 Å, 1.78 Å, 1.17 Å and 1.87 Å respectively (Table 4, Figure 7A). However, the average atomic fluctuation of the flavonoids was also computed which revealed RMSF values for apigenin, biacalein, diadzein, fisetin, genistin, glycitein, phloretin, quercetin and unbound SdiA (Apo) as 1.83 Å, 1.56 Å, 2.05 Å, 2.09 Å, 1.35 Å, 2.85 Å, 1.59 Å, 1.08 Å, and 1.87, respectively (Table 4, Figure 7B).

### 3.7. Binding free energy landscape of SdiA bonded terpene and flavonoid compounds

The binding free energy of the studied SdiA bonded terpenes ranged from -16.6186 kcal/mol to as high as -44.2625 kcal/mol (Table 4). Results revealed that 3,7,11,15-tetramethyl-2-hexadecen-1-ol (phytol) has the highest binding energy of -44.2625 kcal/mol while the least binding energy was observed in P-cymene (-16.6186 kcal/mol) (). For the SdiA bound flavonoids, their binding free energy ranged from -28.8415 kcal/mol to -68.1393 kcal/mol. Genistin showed the highest binding energy of -68.1393 kcal/mol while the least binding energy was observed in Phloretin (-28.8415 kcal/mol) (Table 4).

Results of MM/GBSA-based binding free energy profile of SdiA bonded terpenes and flavonoids revealing other energy components (electrostatic energy, van der Waals energy, solvation free energy and gas-phase free energy) are shown in S2 Table.

### 3.8. Validation of drug likeness properties of the studied terpenes and flavonoids

All the terpenes had 10 heavy atoms (except phytol that had 21), 0 aromatic heavy atoms (except p-cymene that had 6) and Csp<sup>3</sup> fractions of 0.80 (Table 5). The compounds, except for phytol (with higher values) had 0 number of H-bond acceptors and donors with molar refractivity  $\geq 45.22$  and TPSA of 0 Å<sup>2</sup>. On the other hand, flavonoids had heavy atoms and heavy aromatic atoms > 10 with a higher number of H-bond acceptors and donors, Molar refractivity and TPSA  $\geq 4$ , 73 and 70 Å<sup>2</sup> respectively (Table 5).

The consensus Log Po/w of the terpenes was predicted to be  $\geq 3.0$  with phytol having 6.21 while the flavonoids had a value ranging from 0.42–2.3 (Table 5). In the same vein, considering the Log S (Esol and SILICOS-IT), all the terpenes appear to be soluble in water except phytol that appears to be moderately soluble while in the case of the Log S (Ali),  $\alpha$ -pinene and 3-Carene are moderately soluble with poor solubility predicted for phytol. For

Table 5. Drug likeness properties of studied terpenes and flavonoids.

Compounds	Physico-chemical properties				Molar Refractivity	TPSA (Å <sup>2</sup> )	Lipophilicity Consensus Log Po/w	Water Solubility Log S (ESOL)	Class	Pharmacokinetics			Medicinal Chemistry	
	No. heavy atoms	No. rotatable bonds	No. H-bond acceptors	No. H-bond donors						GI absorption	BBB permeation	Log Kp (Skin permeation) (cm/s)	PAINS	Brenk
Phytol	21	13	1	1	98.94	20.23	6.21	-5.98	Moderately soluble	Low	No	-2.29	0 alert	1 alert: isolated_alkene
Beta-pinene	10	0	0	0	45.22	0.00	3.44	-3.31	Soluble	Low	Yes	-4.18	0 alert	1 alert: isolated_alkene
Alpha-pinene	10	0	0	0	45.22	0.00	3.42	-3.51	Soluble	Low	Yes	-3.95	0 alert	1 alert: isolated_alkene
P-cymene	10	1	0	0	45.99	0.00	3.50	-3.63	Soluble	Low	Yes	-4.21	0 alert	0 alert
Alpha-terpinene	10	1	0	0	47.12	0.00	3.30	-3.30	Soluble	Low	Yes	-4.11	0 alert	0 alert
Isoterpinolene	10	0	0	0	47.12	0.00	3.09	-2.90	Soluble	Low	Yes	-4.64	0 alert	0 alert
3-Carene	10	0	0	0	45.22	0.00	3.42	-3.44	Soluble	Low	Yes	-4.02	0 alert	1 alert: isolated_alkene
Sabinene	10	1	0	0	45.22	0.00	3.25	-2.57	Soluble	Low	Yes	-4.94	0 alert	1 alert: isolated_alkene
Camphene	10	0	0	0	45.22	0.00	3.43	-3.34	Soluble	Low	Yes	-4.13	0 alert	1 alert: isolated_alkene
Glycitein	21	2	4	2	78.46	79.90	2.30	-3.57	Soluble	High	No	-6.30	0 alert	0 alert
Phloretin	20	4	5	4	74.02	97.99	1.93	-3.38	Soluble	High	No	-6.11	0 alert	0 alert
Fisetin	21	1	6	4	76.01	111.13	1.55	-3.35	Soluble	High	No	-6.65	1 alert: catecho_A	1 alert: catecho_A
Genistin	31	4	10	6	106.11	170.05	0.42	-3.18	Soluble	Low	No	-8.33	0 alert	0 alert
Apigenin	20	1	5	3	73.99	90.90	2.11	-3.94	Soluble	High	No	-5.80	0 alert	0 alert
Baicalein	20	1	5	3	73.99	90.90	2.24	-4.03	Moderately soluble	High	No	-5.70	1 alert: catecho_A	1 alert: catecho_A
Daidzein	19	1	4	2	71.97	70.67	2.24	-3.53	Soluble	High	Yes	-6.10	0 alert	0 alert
Quercetin	22	1	7	5	78.03	131.36	1.23	-3.16	Soluble	High	No	-7.05	1 alert: catecho_A	1 alert: catecho_A
Furanosylboratedlester	13	0	7	4	37.77	108.61	-2-32	0.48	Highly soluble	Low	No	-9.18	0 alert	1 alert: heavy_metal

the flavonoids, all the compounds were soluble (except baicalein) by the Log S (Esol) parameter while the baicalein, apigenin, genistin, glycitein, daidzein were moderately soluble by the Log S (Ali and SILICOS-IT) solubility values (S3 Table).

Additionally, the terpenes had low gastrointestinal (GI) absorption, are not P-glycoprotein substrates and can permeate the blood-brain barrier (BBB), except phytol with  $\text{Log } K_p \geq 4.0$  cm/s although phytol and  $\alpha$ -pinene had values of  $-2.29$  cm/s and  $-3.95$  cm/s respectively (Table 5). The terpenes were predicted as non-inhibitors of CYP1A2, CYP2C19, CYP3A4 with only P-cymene, alpha-terpinene and sabinene having the potential not to inhibit CYP2C9. In the case of the flavonoids, all the compounds except for genistin showed high GI absorption potential, could not serve as Pgp substrates while only Daidzein can permeate the BBB. The alkaloids had  $\text{Log } K_p > 5.0$  with no inhibitory potentials on CYP2C19 and CYP2C9 (except phloretin) although all the compounds could possibly inhibit the activity of CYP1A2, CYP2D6 and CYP3A4 respectively (S4 Table).

Apart from phytol that disobeyed the Veber and Egan rule, all the terpenes obeyed the rules in addition to Lipinski's although they disobeyed the Ghose and Muegge rules. The flavonoids on the other hand obeyed all the rules except for genistin that violates the Veber, Egan and Muegge rules respectively. Overall, the bioavailability scores of both terpenes and flavonoids were found to be 0.55 F (S5 Table). All the terpenes did not pass the lead likeness test while all flavonoids (except for genistin) scaled through the lead likeness test (S6 Table).

Moreover, the terpenes had zero alert PAINS with zero or one alert brek and synthetic availabilities of  $\geq 1.00$ . In the case of flavonoids, the compounds fisetin, baicalein and quercetin had 1 alert PAINS and brek with catechol A. Other compounds showed 0 alert PAINS and 0 alert brek respectively (Table 5).

#### 4. Discussion

*K. pneumoniae* was studied due to its ability to become progressively resistant to almost all classes of conventional antibiotics (Adeosun et al., 2022). As such, its virulence poses threat to global health, hence, the need to explore the potentials of bioactive compounds as alternative treatment remedies. The present study explored new targets within the bacterial cell that could be modulated by bioactive compounds as potential therapeutic targets and inhibitors to attenuate mild to severe infections (Gorlenko et al., 2020). Since terpenes, commonly found in essential oils and flavonoids possess antimicrobial actions of bacteriostatic and bactericidal effects (Mahizan et al., 2019), they were explored to inhibit virulence factors in *K. pneumoniae*, which is often modulated by SdiA protein. Due to the unavailability of the crystal structure of SdiA protein from *K. pneumoniae* in the structural databases, its 3D model was built using the Swiss model workspace and the quality of the built model was validated. Currently, *in silico* pharmacology paradigm is being explored as a result of its wide range of prospects which speeds up the identification of new targets and eventually result in the development of drugs with anticipated biological activity for these novel targets (Ekins et al., 2007).

Virtual screening strategies such as molecular docking and MDS are often employed for the prediction of the preferred binding orientation of ligands into receptors (Ramírez &

Caballero, 2018). These approaches provide quick insights on the specific targets and compounds that are likely to move from the laboratory to the clinic and eventually to the market as rapidly as possible given the amount of information that needs to be processed for drug discovery (Swaan & Ekins, 2005).

Molecular docking is a technique in drug discovery which is useful in estimating the binding and fitting of two molecular structures. In addition, it reveals the molecular recognition pattern between protein and ligands (Naqvi et al., 2018), hence, it was employed in this study. Findings from our docking studies presented insightful interactions between the test phytocompounds and the SdiA receptor protein, implicated in the expression of virulence in *K. pneumoniae*. Ligand interactions were shown in Figures 4 and 5. Docking results confirmed nine (9) terpenes and eight (8) flavonoids as competitive inhibitors of virulence, vital in the development of therapeutic agents for the management of *K. pneumoniae* infections. Of the studied chemical groups, phytol (-9.205 kcal/mol) and glycitein (-9.752 kcal/mol) had the best docking scores, displaying the highest binding affinity.

The improved binding affinities can be attributed to the test compounds' ability to fit well in the receptor's pocket (Baloyi et al., 2021). Good docking scores observed for these compounds suggest that they are better QSIs which can be characterized by the presence of functional groups. The presence of methoxy and hydroxy functional groups in glycitein structure could have contributed to its good binding property, thereby making it a better QSI as per the criteria stated by Qin et al. (2020). Hydroxyl group is also found in phytol which consists of an oxygen atom covalently linked to a hydrogen atom. The link between oxygen and hydrogen is extremely polar due to the strong electronegativity of the oxygen atom (Swaan & Ekins, 2005). Resulting from this, water molecules are drawn to the hydroxyl group, generating hydrogen bonds which in turn improves the binding affinity. (Chen et al., 2016; Oyewole et al., 2020) documented that 'the higher the binding affinity as observed for phytol and genistin in this study, the more improved the inhibitory effect of the compound'. This presents them as the most potent of all the terpene and flavonoid compounds considered in this study.

Good docking scores were also reported for apigenin (-8.222 kcal/mol), quercetin (-9.290 kcal/mol) and phloretin (-9.722 kcal/mol) in this study. Congruent to our findings, (Vikram et al., 2010) have previously reported apigenin and quercetin as effective antagonists of QS, inhibiting virulence in other GNB such as *Vibrio harveyi* and *Escherichia coli* O157:H7. The good docking scores observed for the tested terpenes and flavonoids imply that they have inhibitory actions that are linked to SdiA binding mechanisms. This also suggests that they may be physiologically active as well as highly efficient molecules, as they provide energy to promote the protein-ligand binding interaction (Gupta & Bajaj, 2018). The direct binding of virulence-associated proteins as observed in this study can be added as potent therapeutic target of flavonoids, in addition to the antibacterial mechanism of action, as also noted by Donadio et al. (2021).

Furthermore, the hydrogen bond interactions observed in some compounds like phytol against the SdiA protein were comparable to furanosyl borate diester (A1-2 molecule) hydrogen bonded with Val57, Arg111, Leu115, Arg116. Glycitein formed hydrogen bonds with Ser43, phloretin with PG4 302 and H<sub>2</sub>O, fisetin with Asp80 and Ser13, genistin with



Asp97 and Trp 95, baicalein with Asp97, daidzein with Ser43 and quercetin with Trp57. According to (Ahmed et al., 2021), the hydrogen bond between a protein and a ligand plays a significant role in their recognition and is often useful in investigating the stability, directionality, and specificity of polar interactions.

Another vital virtual screening tool employed in this study is MDS. MDS helps to study atomic movements of biological systems, and to understand molecular interaction mechanisms (Naqvi et al., 2018). The RMSD and RMSF are the two most widely used metrics of structural fluctuations in MDS which provides insight on inter-atomic motions and stability of the protein-ligand complex (Kuzmanic & Zagrovic, 2010).

RMSD is important for analyzing time-dependent structural motions as well as determining structure's inability to drift away from the initial coordinates over time in simulations (Martínez, 2015). Our study ascertained the overall conformational stability of SdiA protein upon binding to the test compounds by monitoring the RMSD, where RMSD of the bound systems were measured relative to the unbound SdiA structure. Results revealed varying stability of the compounds with RMSD scores ranging between 1.48 Å to 2.58 Å for terpenes and 1.44 Å to 2.50 Å for flavonoids (Table 4). Overall, all the bound compounds (terpenes and flavonoids) stabilized the SdiA conformation as evidenced by the estimated RMSD averages in the range 1.44 Å to 2.58 Å for all bound systems in contrast to the unbound SdiA system after the 100 ns simulation. Notably, sabinene and genistin had the lowest RMSD averages of 1.48 Å and 1.44 Å respectively for the terpenes and flavonoids, correlating to the compounds that enacted the most structural stability. In most structural studies, a higher average RMSD correlates to a less stable structural conformation and vice versa as employed in various studies (Abdullahi et al., 2018; Salifu et al., 2019). According to (Ramírez & Caballero, 2018), RMSD < 2.0 Å corresponds to good docking solutions. Moreover, RMSD scores between 2.0 and 3.0 Å may have deviated from the position of the reference, but they keep the desired orientation. Corroborative to the set rules in (Qin et al., 2020), none of the studied terpenes and flavonoids had RMSD score >3.0 Å.

Furthermore, the displacement of a single atom, or a group of atoms, relative to the reference structure is measured by RMSF, which is averaged across the number of atoms (Farmer et al., 2017). RMSF was calculated in our study to elucidate the flexibility and motion of individual residues in the protein.

The average deviation of the systems was monitored by the RMSF from a reference point over 100 ns. Our findings revealed RMSF scores ranging from 1.08 Å to 3.74 Å for the studied terpenes and flavonoids (Table 4). Overall, quercetin revealed the least RMSF score (1.08 Å), which correspond with the RMSD to depict high stability. The good RMSF score observed may imply that the catalytic machinery in the SdiA active site was not altered by its binding (Martínez, 2015).

The assessment of flexibility of the studied compounds indicates a diverse activity associated with the binding of each compound. This is in reference to some of the compounds (alpha-pinene, alpha-terpinene, 3-carene, phytol, sabinene, apigenin, biacelein, genistin, phloretin and quercetin) exhibiting less flexibility on the SdiA structure while other compounds such as beta-pinene, camphene, isoterpinene, p-cymene, diadzein, fisetin and

glycitein proved to be highly flexible relative to the unbound SdiA state. The substantial difference in structural flexibility of the bound terpenes and flavonoids in contrast to the unbound SdiA could play a crucial role in the biological activity of the protein (Salifu et al., 2019), as the binding of the compounds may result in a more flexible or more rigid SdiA structure which directly impacts the native state of the protein.

The molecular mechanics/Poisson Boltzmann surface area (MM/PBSA) and the molecular mechanics/generalized-born surface area combine molecular mechanics computations with continuum solvation models to derive binding free energies for macromolecules (Hou et al., 2011). They serve as powerful tools in drug design where a correct ranking of inhibitors is often emphasized (Hou et al., 2011). Hence, the approach which represents a higher-level scoring theory than docking was used to estimate the aggregate binding free energy of the compound complexes as presented in Table 4. Genistin revealed the highest binding free energy score of  $-68.1393$  kcal/mol for flavonoids while phytol revealed  $-44.2625$  kcal/mol as the highest for terpenes. These calculated energies provide comprehensive molecular-level evidence that could be useful to design a drug by creating better ligand binding.

In addition, certain parameters of the selected terpenes and flavonoids were predicted for their physicochemical properties, lipophilicity, water-solubility, pharmacokinetics, drug-likeness and medicinal chemistry. In this study, the drug likeness properties were characterized to determine the pharmacokinetics of the test compounds, by testing for favorable ADME (absorption, distribution, metabolism, and excretion) properties. A major criterion employed for the characterization was hinged on the lipinski rule of five. This rule predicts the poor absorption or permeation of a drug when there are more than 5 hydrogen bond donors, 10 hydrogen bond acceptors, molecular weight larger than 500, and an estimated Log P (CLog P) value greater than 5 (Benet et al., 2016). Results of this assessment revealed that the test compounds obeyed the rules, with glycitein, phloretin, quercetin, fisetin, apigenin, alpha terpinene, isoterpinolene, biacalein and daidzein having no violation. However, phytol, genistin, beta pinene, alpha pinene, p-cymene, 3-carene, sabinene and camphene only showed one violation each, which is considered acceptable since the violation does not exceed one, a submission opined by Pathania and Singh (2021). This result suggests the potential drug-likeness features of the compounds. Drug likeness can often be used as a proxy for oral bioavailability especially because bioavailability is amongst the most prominent criteria of a drug (Bickerton et al., 2012). Heavy atoms were also observed in the test compounds. The presence of heavy atoms in compounds is an important chemical structure-related character linked to their physicochemical properties and drug-likeness properties (Mao et al., 2016). Other pharmacokinetic principles such as ghose filter, veber filter, egan filter and muegge filter also supported the drug likeness characteristics of the test compounds as shown in S5 Table. These principles are accepted by researchers as one of the key evaluation parameters for the drug-likeness of any virtually screened molecule (Pathania & Singh, 2021).

Another interesting finding from this study is that all the terpenes studied but phytol can permeate the blood-brain barrier (BBB) (Table 2), suggesting their potential to permeate the central nervous system (CNS) which is indicative of therapeutic ability. This corroborates the submission of Agatonovic-Kustrin et al. (2019) who opined that many terpenes could cross the BBB. From the flavonoids tested, daidzein revealed the ability to permeate the BBB,

possibly due to its broad therapeutic activities which include cardioprotective, anticancer, anti-allergic, antidiabetic, anti-inflammatory and anti-oxidative properties as reported by Kwiecień et al. (2020). Stout et al. (2013) corroborates that daidzein can cross the BBB in mice, and to improve cognition, reduce anxiety, aggression, and increase locomotory movement.

In medicinal chemistry, the Brenk and pan assay interference compounds (PAINS) structural alerts predict unstable, reactive, toxic fragments present in the structure (Sultan et al., 2020). All active compounds, except fisetin, baicalein and quercetin had zero alerts in PAINS descriptors (Table 5), providing added promising indicators as drug candidates. Physicochemical characteristics are critical in the efficiency, care, and absorption of compounds (Meanwell, 2011).

Thus far, the *in-silico* results demonstrate phytol, genistin and glycitein as the best compounds bound to the modeled SdiA receptor protein, revealed high binding energies, demonstrated stability and less fluctuation in the atomic and inter-atomic interactions in the protein-ligand system, showed drug-like properties as well as moderate solubility in water. The ability of the studied compounds to inhibit virulence activities in *K. pneumoniae* have been elucidated *in vitro*. Results of the *in vitro* studies validated the *in-silico* findings, proving the compounds to be promising in the development of drugs against *K. pneumoniae* infections.

## 5. Conclusions

The continuous emergence of MDR *K. pneumoniae* necessitates the search to explore natural products of plant origin as pivotal in the management of its infections. This study validated p-cymene, alpha-pinene, isoterpinolene, alpha-terpinene, phytol, 3-carene, beta-pinene, sabinene, camphene, fisetin, genistin, diadzein, quercetin, glycitein, phloretin, apigenin and baicalein (terpenes and flavonoids) bound SdiA's autoinducer binding site forming critical interactions with the binding site's key residues. The MDS established the inhibitory performance and interactions revealing free binding energies as high as  $-68.1393$  kcal/mol for genistin (flavonoid) and  $-44.2625$  kcal/mol for phytol (terpene). The drug-likeness prediction of the selected compounds validated their drug potential conferring them as promising QSI drugs for *K. pneumoniae*. Therefore, the study further suggests the exploration of terpenes and flavonoids as alternative QSIs, other than the known antibacterial target sites.

## Acknowledgments

The authors acknowledge Professor Zeno Apostolides from the Division of Biochemistry, Department of Biochemistry, Genetics and Microbiology, the University of Pretoria for providing us with the Schrödinger package software and the Centre for High-Performance Computing (CHPC), Cape Town, South Africa.

## Disclosure statement

No potential conflict of interest was reported by the authors.

## Authors' contributions

Conceptualization: Sekelwa Cosa; Data curation and investigation: Idowu J. Adeosun, Aimen K. Aljoundi, Mohammed A. Ibrahim, Elliasu Y. Salifu; Methodology: Idowu J. Adeosun, Itumeleng T. Baloyi, Aimen K. Aljoundi, Mohammed A. Ibrahim, Elliasu Y. Salifu; Supervision: Sekelwa Cosa; Writing—original draft: Idowu J. Adeosun; Writing—review and editing: Idowu J. Adeosun, Itumeleng T. Baloyi, Elliasu Y. Salifu, Sekelwa Cosa; Funding and resources acquisition: Sekelwa Cosa.

## Funding

This research was funded in parts by the South African Medical Research Council–Self Initiated Research (SAMRC-SIR) to S.C.

## Abbreviations

WHO	World Health Organization
MDR	Multidrug-resistance
UTIs	Urinary tract infections
QS	Quorum sensing
QSIs	Quorum sensing inhibitors
GNB	Gram-negative bacteria
AIs	autoinducers
AHLs	N-acyl-homoserine lactones
MD	Molecular docking
MDS	Molecular dynamics simulation
SdiA	Suppressor of cell division inhibition
MMV	Molegro Molecular Viewer
MM/PB-SA	Molecular Mechanics/Poisson-Boltzmann Surface Area
BBB	Blood-brain barrier
PAINS	Pan-assay interference compounds
TPSA	Topological polar surface area.

## References

- Abdullahi, M., Olotu, F. A., & Soliman, M. E. (2018). Allosteric inhibition abrogates dysregulated LFA-1 activation: Structural insight into mechanisms of diminished immunologic disease. *Computational Biology and Chemistry*, *73*, 49–56. <https://doi.org/10.1016/j.compbiolchem.2018.02.002>
- Adeosun, I. J., Baloyi, I. T., & Cosa, S. (2022). Anti-biofilm and associated anti-virulence activities of selected phytochemical compounds against *Klebsiella pneumoniae*. *Plants*, *11*(11), 1429. <https://doi.org/10.3390/plants11111429>
- Adeosun, I. J., Oladipo, E. K., Ajibade, O. A., Olotu, T. M., Oladipo, A. A., Awoyelu, E. H., Alli, O. A. T., & Oyawoye, O. M. (2019). Antibiotic susceptibility of *Klebsiella pneumoniae* isolated from selected tertiary hospitals in Osun state, Nigeria. *Iraqi Journal of Science*, *60*(7), 1423–1429. <https://doi.org/10.24996/ij.s.2019.60.7.2>
- Agatonovic-Kustrin, S., Kustrin, E., & Morton, D. W. (2019). Essential oils and functional herbs for healthy aging. *Neural Regeneration Research*, *14*(3), 441–445. <https://doi.org/10.4103/1673-5374.245467>
- Ahmed, M. Z., Muteeb, G., Khan, S., Alqahtani, A. S., Somvanshi, P., Alqahtani, M. S., Ameta, K. L., & Haque, S. (2021). Identifying novel inhibitor of quorum sensing transcriptional regulator (SdiA) of *Klebsiella pneumoniae* through modelling, docking and molecular dynamics simulation. *Journal of Biomolecular Structure and Dynamics*, *39*(10), 3594–3604. <https://doi.org/10.1080/07391102.2020.1767209>
- Akinyede, K. A., Ekpo, O. E., & Oguntibeju, O. O. (2020). Ethnopharmacology, therapeutic properties and nutritional potentials of *Carpobrotus edulis*: A comprehensive review. *Scientia Pharmaceutica*, *88*(3), 39. <https://doi.org/10.3390/scipharm88030039>
- Allouche, A. (2011). Software news and updates. Gabedit—A graphical user interface for computational chemistry softwares. *Journal of Computational Chemistry*, *32*(1), 174–182. <https://doi.org/10.1002/jcc>
- Almeida, F. A. d., Pinto, U. M., & Vanetti, M. C. D. (2016). Novel insights from molecular docking of SdiA from *Salmonella enteritidis* and *Escherichia coli* with quorum sensing and quorum quenching molecules. *Microbial Pathogenesis*, *99*, 178–190. <https://doi.org/10.1016/j.micpath.2016.08.024>
- Arnold, K., Bordoli, L., Kopp, J., & Schwede, T. (2006). The SWISS-MODEL workspace: A web-based environment for protein structure homology modelling. *Bioinformatics (Oxford, England)*, *22*(2), 195–201. <https://doi.org/10.1093/bioinformatics/bti770>
- Baloyi, I. T., Adeosun, I. J., Yusuf, A. A., & Cosa, S. (2021). *In silico* and *in vitro* screening of antipathogenic properties of *Melianthus comosus* (Vahl) against *Pseudomonas aeruginosa*. *Antibiotics*, *10*(6), 679. <https://doi.org/10.3390/antibiotics10060679>

- Baloyi, I. T., Cosa, S., Combrinck, S., Leonard, C. M., & Viljoen, A. M. (2019). Anti-quorum sensing and antimicrobial activities of South African medicinal plants against uropathogens. *South African Journal of Botany*, *122*, 484–491. <https://doi.org/10.1016/j.sajb.2019.01.010>
- Benet, L. Z., Hosey, C. M., Ursu, O., & Oprea, T. I. (2016). BDDCS, the Rule of 5 and drugability. *Advanced Drug Delivery Reviews*, *101*, 89–98. <https://doi.org/10.1016/j.addr.2016.05.007>
- Bergman, M. E., Davis, B., & Phillips, M. A. (2019). Medicinal useful plant terpenoids: Biosynthesis, occurrence, and mechanism of action. *Molecules*, *24*(21), 3961. <https://doi.org/10.3390/molecules24213961>
- Bickerton, G. R., Paolini, G. V., Besnard, J., Muresan, S., & Hopkins, A. L. (2012). Quantifying the chemical beauty of drugs Europe PMC Funders Group. *Nature Chemistry*, *4*(2), 90–98. <https://doi.org/10.1038/nchem.1243>. Quantifying
- Boucher, H. W., Talbot, G. H., Bradley, J. S., Edwards, J. E., Gilbert, D., Rice, L. B., Scheld, M., Spellberg, B., & Bartlett, J. (2009). Bad bugs, no drugs: No ESCAPE! An update from the Infectious Diseases Society of America. *Clinical Infectious Diseases*, *48*(1), 1–12. <https://doi.org/10.1086/595011>
- Cadavid, E., Robledo, S. M., Quiñones, W., & Echeverri, F. (2018). Induction of biofilm formation in *Klebsiella pneumoniae* ATCC 13884 by several drugs: The possible role of quorum sensing modulation. *Antibiotics*, *7*(4), 103–114. <https://doi.org/10.3390/antibiotics7040103>
- Chen, D., Oezguen, N., Urvil, P., Ferguson, C., Dann, S. M., & Savidge, T. C. (2016). Regulation of protein-ligand binding affinity by hydrogen bond pairing. *Science Advances*, *2*(3), e1501240. <https://doi.org/10.1126/sciadv.1501240>
- Cheng, C., Yan, X., Liu, B., Jiang, T., Zhou, Z., Zhang, D., Wang, H., Chen, D., Li, C., Fang, T., Agriculture, F., & Province, F. (2022). SdiA, a quorum sensing transcriptional regulator, enhanced the drug resistance of *Cronobacter sakazakii* and suppressed its motility, adhesion and biofilm formation. *Frontiers in Microbiology*, *13*, 1–14. <https://doi.org/10.3389/fmicb.2022.901912>
- Cosa, S., Chaudhary, S. K., Chen, W., Combrinck, S., & Viljoen, A. (2019). Exploring common culinary herbs and spices as potential anti-quorum sensing agents. *Nutrients*, *11*(4), 739. <https://doi.org/10.3390/nu11040739>
- Cosa, S., Rakoma, J. R., Yusuf, A. A., & Tshikalange, T. E. (2020). *Calpurnia aurea* (Aiton) benth extracts reduce quorum sensing controlled virulence factors in *Pseudomonas aeruginosa*. *Molecules*, *25*(10), 2283. <https://doi.org/10.3390/molecules25102283>
- Cox-Georgian, D., Ramadoss, N., Dona, C., & Basu, C. (2019). Therapeutic and medicinal uses of terpenes. In *Medicinal plants: From farm to pharmacy*, 333–359. [https://doi.org/10.1007/978-3-030-31269-5\\_15](https://doi.org/10.1007/978-3-030-31269-5_15)

Daina, A., Michielin, O., & Zoete, V. (2017). SwissADME: A free web tool to evaluate pharmacokinetics, drug-likeness and medicinal chemistry friendliness of small molecules. *Scientific Reports*, 7, 42717. <https://doi.org/10.1038/srep42717>

Donadio, G., Mensitieri, F., Santoro, V., Parisi, V., Bellone, M. L., De Tommasi, N., Izzo, V., & Piaz, F. D. (2021). Interactions with microbial proteins driving the antibacterial activity of flavonoids. *Pharmaceutics*, 13(5), 660. <https://doi.org/10.3390/pharmaceutics13050660>

Ekins, S., Mestres, J., & Testa, B. (2007). *In silico* pharmacology for drug discovery: Applications to targets and beyond. *British Journal of Pharmacology*, 152(1), 21–37. <https://doi.org/10.1038/sj.bjp.0707306>

Farmer, J., Kanwal, F., Nikulsin, N., Tsilimigras, M. C. B., & Jacobs, D. J. (2017). Statistical measures to quantify similarity between molecular dynamics simulation trajectories. *Entropy*, 19(12), 646. <https://doi.org/10.3390/e19120646>

Gonnet, P. (2007). P-SHAKE: A quadratically convergent SHAKE in  $O(n^2)$ . *Journal of Computational Physics*, 220(2), 740–750. <https://doi.org/10.1016/j.jcp.2006.05.032>

Gopu, V., & Shetty, P. H. (2016). Cyanidin inhibits quorum signalling pathway of a food borne opportunistic pathogen. *Journal of Food Science and Technology*, 53(2), 968–976. <https://doi.org/10.1007/s13197-015-2031-9>

Gorlenko, C. L., Kiselev, H. Y., Budanova, E. V., Zamyatnin, A. A., & Ikryannikova, L. N. (2020). Plant secondary metabolites in the battle of drugs and drug-resistant bacteria: New heroes or worse clones of antibiotics? *Antibiotics*, 9(4), 170. <https://doi.org/10.3390/antibiotics9040170>

Gupta, S., & Bajaj, A. V. (2018). Extra precision glide docking, free energy calculation and molecular dynamics studies of 1,2-diarylethane derivatives as potent urease inhibitors. *Journal of Molecular Modeling*, 24(9), 261. <https://doi.org/10.1007/s00894-018-3787-4>

Homeyer, N., & Gohlke, H. (2012). Free energy calculations by the molecular mechanics Poisson-Boltzmann surface area method. *Molecular Informatics*, 31(2), 114–122. <https://doi.org/10.1002/minf.201100135>

Hou, T., Wang, J., Li, Y., & Wang, W. (2011). Assessing the performance of the MM/PBSA and MM/GBSA methods. 1. The accuracy of binding free energy calculations based on molecular dynamics simulations. *Journal of Chemical Information and Modeling*, 51(1), 69–82. <https://doi.org/10.1021/ci100275a>

Huggins, D. J., Venkitaraman, A. R., & Spring, D. R. (2011). Rational methods for the selection of diverse screening compounds. *ACS Chemical Biology*, 6(3), 208–217. <https://doi.org/10.1021/cb100420r>

Koh, C., Sam, C., Yin, W., Tan, L. Y., Krishnan, T., Chong, Y. M., & Chan, K. (2013). Plant-derived natural products as sources of anti-quorum sensing compounds. *Sensors (Basel, Switzerland)*, 13(5), 6217–6228. <https://doi.org/10.3390/s130506217>

- Kusumaningrum, S., Budianto, E., Kosela, S., Sumaryono, W., & Juniarti, F. (2014). The molecular docking of 1,4-naphthoquinone derivatives as inhibitors of Polo-like kinase 1 using Molegro Virtual Docker. *Journal of Applied Pharmaceutical Science*, *4*(11), 47–53. <https://doi.org/10.7324/JAPS.2014.4119>
- Kuzmanic, A., & Zagrovic, B. (2010). Determination of ensemble-average pairwise root mean-square deviation from experimental B-factors. *Biophysical Journal*, *98*(5), 861–871. <https://doi.org/10.1016/j.bpj.2009.11.011>
- Kwiecień, A., Ruda-Kucerova, J., Kamiński, K., Babinska, Z., Popiołek, I., Szczubiałka, K., Nowakowska, M., & Walczak, M. (2020). Improved pharmacokinetics and tissue uptake of complexed Daidzein in rats. *Pharmaceutics*, *12*(2), 162. <https://doi.org/10.3390/pharmaceutics12020162>
- Laskowski, R. A., Jabłońska, J., Pravda, L., Vařeková, R. S., & Thornton, J. M. (2018). PDBsum: Structural summaries of PDB entries. *Protein Science*, *27*(1), 129–134. <https://doi.org/10.1002/pro.3289>
- Lee, T. S., Cerutti, D. S., Mermelstein, D., Lin, C., Legrand, S., Giese, T. J., Roitberg, A., Case, D. A., Walker, R. C., & York, D. M. (2018). GPU-accelerated molecular dynamics and free energy methods in amber18: Performance enhancements and new features. *Journal of Chemical Information and Modeling*, *58*(10), 2043–2050. <https://doi.org/10.1021/acs.jcim.8b00462>
- Madhavi Sastry, G., Adzhigirey, M., Day, T., Annabhimoju, R., & Sherman, W. (2013). Protein and ligand preparation: Parameters, protocols, and influence on virtual screening enrichments. *Journal of Computer-Aided Molecular Design*, *27*(3), 221–234. <https://doi.org/10.1007/s10822-013-9644-8>
- Mahizan, N. A., Yang, S.-K., Moo, C.-L., Song, A. A.-L., Chong, C.-M., Chong, C.-W., Abushelaibi, A., Lim, S.-H. E., & Lai, K.-S. (2019). Terpene derivatives as a potential agent against antimicrobial resistance. *Molecules*, *24*(14), 2631. <https://doi.org/10.3390/molecules24142631>
- Maier, J. A., Martinez, C., Kasavajhala, K., Wickstrom, L., Hauser, K. E., & Simmerling, C. (2015). ff14SB: Improving the accuracy of protein side chain and backbone parameters from ff99SB. *Journal of Chemical Theory and Computation*, *11*(8), 3696–3713. <https://doi.org/10.1021/acs.jctc.5b00255>
- Mao, F., Ni, W., Xu, X., Wang, H., Wang, J., Ji, M., & Li, J. (2016). Chemical structure-related drug-like criteria of global approved drugs. *Molecules (Basel, Switzerland)*, *21*(1), 75. <https://doi.org/10.3390/molecules21010075>
- Maroyi, A. (2017). Review of ethnomedicinal uses, phytochemistry and pharmacological properties of *Euclea natalensis* A.DC. *Molecules*, *22*(12), 2128. <https://doi.org/10.3390/molecules22122128>



- Martínez, L. (2015). Automatic identification of mobile and rigid substructures in molecular dynamics simulations and fractional structural fluctuation analysis. *PLoS One*, *10*(3), e0119264. <https://doi.org/10.1371/journal.pone.0119264>
- Meanwell, N. A. (2011). Improving drug candidates by design: A focus on physicochemical properties as a means of improving compound disposition and safety. *Chemical Research in Toxicology*, *24*(9), 1420–1456. <https://doi.org/10.1021/tx200211v>
- Naqvi, A. A. T., Mohammad, T., Hasan, G. M., & Hassan, M. I. (2018). Advancements in docking and molecular dynamics simulations towards ligand-receptor interactions and structure-function relationships. *Current Topics in Medicinal Chemistry*, *18*(20), 1755–1768. <https://doi.org/10.2174/1568026618666181025114157>
- Nikitin, S. (2014). *Leap gradient algorithm* (pp. 1–24). <http://arxiv.org/abs/1405.5548>
- Oleg, T., & Arthur, O. (2010). Software news and updates gabedit - a graphical user interface for computational chemistry softwares. *Journal of Computational Chemistry*, *32*, 174-182. <https://doi.org/10.1002/jcc>
- Oyewole, R. O., Oyebamiji, A. K., & Semire, B. (2020). Theoretical calculations of molecular descriptors for anticancer activities of 1, 2, 3-triazole-pyrimidine derivatives against gastric cancer cell line (MGC-803): DFT, QSAR and docking approaches. *Heliyon*, *6*(5), e03926. <https://doi.org/10.1016/j.heliyon.2020.e03926>
- Pacheco, T., Gomes, A. É. I., Siqueira, N. M. G., Assoni, L., Darrieux, M., Venter, H., & Ferraz, L. F. C. (2021). SdiA, a quorum-sensing regulator, suppresses fimbriae expression, biofilm formation, and quorum-sensing signaling molecules production in *Klebsiella pneumoniae*. *Frontiers in Microbiology*, *12*, 597735. <https://doi.org/10.3389/fmicb.2021.597735>
- Paczkowski, J. E., Mukherjee, S., McCreedy, A. R., Cong, J. P., Aquino, C. J., Kim, H., Henke, B. R., Smith, C. D., & Bassler, B. L. (2017). Flavonoids suppress *Pseudomonas aeruginosa* virulence through allosteric inhibition of quorum-sensing receptors. *The Journal of Biological Chemistry*, *292*(10), 4064–4076. <https://doi.org/10.1074/jbc.M116.770552>
- Panche, A. N., Diwan, A. D., & Chandra, S. R. (2016). Flavonoids: An overview. *Journal of Nutritional Science*, *5*, e47. <https://doi.org/10.1017/jns.2016.41>
- Pathania, S., & Singh, P. K. (2021). Analyzing FDA-approved drugs for compliance of pharmacokinetic principles: Should there be a critical screening parameter in drug designing protocols? *Expert Opinion on Drug Metabolism & Toxicology*, *17*(4), 351–354. <https://doi.org/10.1080/17425255.2021.1865309>
- Pettersen, E. F., Goddard, T. D., Huang, C. C., Couch, G. S., Greenblatt, D. M., Meng, E. C., & Ferrin, T. E. (2004). UCSF Chimera - A visualization system for exploratory research and analysis. *Journal of Computational Chemistry*, *25*(13), 1605–1612. <https://doi.org/10.1002/jcc.20084>

- Pradeep, C., Lalitha, S., Rajesh, S. V., & Shanmugam, G. (2018). Comparative modeling and molecular docking studies of quorum sensing transcriptional regulating factor Sdia from *Klebsiella pneumoniae*. *International Journal of Current Research in Science, Engineering & Technology*, 1(1), 09. <https://doi.org/10.30967/ijcrset.1.1.2018.9-16>
- Qin, X., Vila-Sanjurjo, C., Singh, R., Philipp, B., & Goycoolea, F. M. (2020). Screening of bacterial quorum sensing inhibitors in a *Vibrio fischeri* LuxR-based synthetic fluorescent *E. coli* biosensor. *Pharmaceuticals*, 13(9), 263. <https://doi.org/10.3390/ph13090263>
- Ramírez, D., & Caballero, J. (2018). Is it reliable to take the molecular docking top scoring position as the best solution without considering available structural data? *Molecules*, 23(5), 1038. <https://doi.org/10.3390/molecules23051038>
- Roe, D. R., & Cheatham, T. E. (2013). PTRAJ and CPPTRAJ: Software for processing and analysis of molecular dynamics trajectory data. *Journal of Chemical Theory and Computation*, 9(7), 3084–3095. <https://doi.org/10.1021/ct400341p>
- Salifu, E. Y., Agoni, C., Olotu, F. A., Dokurugu, Y. M., & Soliman, M. E. S. (2019). Halting ionic shuttle to disrupt the synthetic machinery—structural and molecular insights into the inhibitory roles of bedaquiline towards *Mycobacterium tuberculosis* ATP synthase in the treatment of tuberculosis. *Journal of Cellular Biochemistry*, 120(9), 16108–16119. <https://doi.org/10.1002/jcb.28891>
- Seifert, E. (2014). OriginPro 9.1: Scientific data analysis and graphing software - Software review. *Journal of Chemical Information and Modeling*, 54(5), 1552. <https://doi.org/10.1021/ci500161d>
- Stout, J. M., Knapp, A. N., Banz, W. J., Wallace, D. G., & Cheatwood, J. L. (2013). Subcutaneous daidzein administration enhances recovery of skilled ladder rung walking performance following stroke in rats. *Behavioural Brain Research*, 256, 428–431. <https://doi.org/10.1016/j.bbr.2013.08.027>
- Sultan, M. A., Galil, M. S. A., Al-Qubati, M., Omar, M. M., & Barakat, A. (2020). Synthesis, molecular docking, druglikeness analysis, and ADMET prediction of the chlorinated ethanoanthracene derivatives as possible antidepressant agents. *Applied Sciences (Switzerland)*, 10(21), 7727. <https://doi.org/10.3390/app10217727>
- Sundaresan, K., & Tharini, K. (2018). Identification of potent Cyanoacetylhydrazone derivatives as antidiabetic activity by *in silico* method. *Asian Journal of Pharmacy and Pharmacology*, 4(6), 771–776. <https://doi.org/10.31024/ajpp.2018.4.6.8>
- Swaan, P. W., & Ekins, S. (2005). Reengineering the pharmaceutical industry by crash-testing molecules. *Drug Discovery Today*, 10(17), 1191–1200. [https://doi.org/10.1016/S1359-6446\(05\)03557-9](https://doi.org/10.1016/S1359-6446(05)03557-9)
- Talebi Bezmin Abadi, A., Rizvanov, A. A., Haertlé, T., & Blatt, N. L. (2019). World Health Organization report: Current crisis of antibiotic resistance. *BioNanoScience*, 9(4), 778–788. <https://doi.org/10.1007/s12668-019-00658-4>

- Tavío, M. M., Aquili, V. D., Poveda, J. B., Antunes, N. T., Sánchez-Céspedes, J., & Vila, J. (2010). Quorum-sensing regulator sdiA and marA overexpression is involved in *in vitro*-selected multidrug resistance of *Escherichia coli*. *The Journal of Antimicrobial Chemotherapy*, *65*(6), 1178–1186. <https://doi.org/10.1093/jac/dkq112>
- Thomsen, R., & Christensen, M. H. (2006). MolDock: A new technique for high-accuracy molecular docking. *Journal of Medicinal Chemistry*, *49*(11), 3315–3321. <https://doi.org/10.1021/jm051197e>
- Tian, W., Chen, C., Lei, X., Zhao, J., & Liang, J. (2018). CASTp 3.0: Computed atlas of surface topography of proteins. *Nucleic Acids Research*, *46*(W1), W363–W367. <https://doi.org/10.1093/nar/gky473>
- Tzouveleakis, L. S., Markogiannakis, A., Psychogiou, M., Tassios, P. T., & Daikos, G. L. (2012). Carbapenemases in *Klebsiella pneumoniae* and other *Enterobacteriaceae*: An evolving crisis of global dimensions. *Clinical Microbiology Reviews*, *25*(4), 682–707. <https://doi.org/10.1128/CMR.05035-11>
- Ventola, C. L. (2015). The Antibiotics. *Comprehensive Biochemistry*, *11*(4), 181–224. <https://doi.org/10.1016/B978-1-4831-9711-1.50022-3>
- Vikram, A., Jayaprakasha, G. K., Jesudhasan, P. R., Pillai, S. D., & Patil, B. S. (2010). Suppression of bacterial cell-cell signalling, biofilm formation and type III secretion system by citrus flavonoids. *Journal of Applied Microbiology*, *109*(2), 515–527. <https://doi.org/10.1111/j.1365-2672.2010.04677.x>
- Wang, J., Wolf, R. M., Caldwell, J. W., Kollman, P. A., & Case, D. A. (2004). Development and testing of a general Amber force field. *Journal of Computational Chemistry*, *25*(9), 1157–1174. <https://doi.org/10.1002/jcc.20035>